1985

A finite element stream-aquifer model

Robert Sidney Carr
Iowa State University

A finite element stream-aquifer model

by

Robert Sidney Carr

A Dissertation Submitted to the
Graduate Faculty in Partial Fulfillment of the
Requirements for the Degree of
DOCTOR OF PHILOSOPHY

Department: Civil Engineering
Major: Water Resources

Approved:

Signature was redacted for privacy.

In Charge of Major Work

Signature was redacted for privacy.

For the Major Department

Signature was redacted for privacy.

For the Graduate College

Iowa State University
Ames, Iowa

1985

TABLE OF CONTENTS

	Page
COMMONLY USED SYMBOLS	vii
INTRODUCTION	1
REVIEW OF LITERATURE	3
The Finite Element Method in Groundwater Hydrology	3
Other Groundwater Models	7
EQUATION OF GROUNDWATER FLOW	9
Finite Element Formulation	10
The method of weighted residuals	10
Conversion to Solvable Form	12
Basis Functions and Finite Elements	14
Numerical Integration	16
Maximum Time Step	16
Solution of the System of Equations	17
Solution for an Unconfined Aquifer	18
PRECIPITATION TRANSPORT MODEL	23
Infiltration Model	23
Prediction of Green-Ampt Parameters	27
Sub-Surface Model	29
Evapotranspiration	32
PUMPING WELLS AND STREAMFLOW	34
Pumping Wells	34
Streams	35

MICRO-COMPUTER IMPLEMENTATION 39

ANALYTICAL CALIBRATION 41

TWO DIMENSIONAL MODEL 45

Ames Aquifer Area 45

Calibration to Ames Aquifer Data 48

Verification 53

Southeast Well Field 56

Conclusions 61

Recommendations 64

THREE DIMENSIONAL MODEL 66

Study Area 66

Three Dimensional Pump Test 70

Calibration to Low-Flow Data 72

Calibration to Rainfall Data 77

Conclusions 82

Recommendations 82

CONCLUSIONS AND RECOMMENDATIONS 84

Conclusions 84

Recommendations 84

REFERENCES 86

ACKNOWLEDGEMENTS 90

APPENDIX : BOREHOLE LOG AT THREE DIMENSIONAL WELL SITE 91

LIST OF FIGURES

		Page
Figure 1.	Isoparametric hexahedral elements in global (x,y,z) and local (ξ,η,ζ) coordinates (after Lapidus and Pinder, 1982)	16
Figure 2.	Deformation of finite element mesh with change in the free surface	19
Figure 3.	Infiltration - Storage unsaturated zone model	30
Figure 4.	Variation in outflow from the Soil-Storage model with 'C' parameter	32
Figure 5.	Cross section showing the relationship between head on the aquifer side of the riverbed and head in the stream element (cell). Head in the element is equal to the water-table elevation (after McDonald and Harbaugh, 1983)	38
Figure 6.	Two dimensional finite element mesh applied to transient heat conduction problem	42
Figure 7.	Variation of U with time at node 1 for transient heat conduction problem	44
Figure 8.	Ames area with observation wells and aquifer boundaries	46
Figure 9.	Extent of unconfined portions of the Ames aquifer (after Willie, 1984)	47
Figure 10.	Finite element mesh of Ames aquifer	49
Figure 11.	Asgrow pump test calibration	54
Figure 12.	Drawdown in meters for Ames scenario #1	58
Figure 13.	Drawdown in meters for Ames scenario #2	59
Figure 14.	Drawdown in meters for Ames scenario #3	60
Figure 15.	Drawdown in meters for Ames scenario #4	62

Figure 16.	Drawdown in meters for Ames scenario #5	63
Figure 17.	Location of three dimensional study area	67
Figure 18.	Detail of the three dimensional study area	68
Figure 19.	Detail of piezometers for three dimensional study	69
Figure 20.	Three dimensional mesh in horizontal (x-y) plane	72
Figure 21.	Cross section of three dimensional mesh in East-West direction	73
Figure 22.	Final calibrated aquifer parameters for low-flow data	75
Figure 23.	Calibration plot of three dimensional model to low-flow data	76
Figure 24.	Calibration plot of three dimensional model to rainfall data	79
Figure 25.	Water table levels at peak levels	80
Figure 26.	Equipotential plot at groundwater hydrograph peak for East-West cross section	81
Figure A.1.	Borehole log	93

LIST OF TABLES

		Page
Table 1.	Convergence of the Free Surface Iterative Scheme	22
Table 2.	Range of saturated hydraulic conductivity values (after Bouwer, 1978)	28
Table 3.	Typical Green-Ampt IMD values (after Huber et al., 1982)	29
Table 4.	Typical values of Su (after Huber et al., 1982)	29
Table 5.	Comparison of FEM solution with analytical solution to two-dimensional steady state heat conduction problem	43
Table 6.	Calibration to Akhavi (1970) Pumping Data	50
Table 7.	Water levels at the end of six month no-flow simulation in meters above MSL	55
Table 8.	Groundwater recovery data	55
Table 9.	Pump test drawdown data	71
Table A.1.	Description of borehole log	92

COMMONLY USED SYMBOLS

t	-	time
x,y,z	-	cartesian coordinates
∇	-	gradient operator

INTRODUCTION

The use of numerical models for solving aquifer management problems has become an accepted hydrologic practice in the past decade. Current models written for large computers cannot be easily converted for use on desktop computers because of operating system and language implementation differences. Furthermore, the new desktop machines tend to be far more interactive than the traditional batch process computers and thus the advantages of the new machines would be lost if existing models were converted. A need was seen to develop a set of general purpose groundwater aquifer management tools specifically designed for the micro computer environment. The models were to be designed with a modular structure. Modularity allows the program to be designed so that all hydrologic inputs are independent. This allows the model to be easily altered later if needed. Pascal is a block structured language typical of modern computer languages, and thus is ideally suited to a modular program design.

The use of finite element techniques in groundwater hydrology has greatly increased in the past few years. Many researchers have created models for specific hydrologic problems, but unfortunately, no readily available general purpose models exist. This research uses finite element techniques to model the groundwater flow equations in a

general purpose format. By general purpose, it is meant that the model may be applied to any problem without code modification. The only responsibilities of the user are correct data inputs.

The models described in this dissertation are continuous simulation models able to simulate both confined and unconfined aquifer systems. Hydrologic variables such as pumping, stream flow, infiltration and evapotranspiration are also modeled. In addition, both two dimensional and three dimensional flow models are available so that specific aquifer geometries may be correctly simulated.

The models are first calibrated to analytical solutions, thereby proving mathematical correctness. An important step in the introduction of any new groundwater model is the correct calibration and verification of the models. To this end, the Ames aquifer (a shallow aquifer system in Ames, Iowa) was used to calibrate and verify both the two and three dimensional models. Three dimensional data were collected for the calibration and verification of the three dimensional model.

REVIEW OF LITERATURE

The following review of literature is intended as an overview of the finite element method in groundwater simulation with specific reference to three dimensional modeling. Some techniques from other areas of mechanics relevant to this thesis are discussed.

The Finite Element Method in Groundwater Hydrology

The use of finite elements to model groundwater problems has been a relatively recent development. Until the late 1960s, finite difference procedures were generally used to solve for situations where analytical solution was impossible. Unfortunately, the finite difference method becomes extremely cumbersome to use in three dimensional models when flow with a free surface is involved. The very nature of the finite element method makes it ideally suited to problems in which the geometry must be changed frequently. Furthermore, most finite difference groundwater models average pumping rates over finite areas which is exactly the concept of the finite element method. One of the great advantages of the finite element method is that complex boundary geometries may be approximated by variable geometry isoparametric elements. The isoparametric transformation allows complex element geometries to be used without difficulty. Another advantage is that each finite element may be defined by many points. This type of

element allows the groundwater solution to be approximated by piecewise high order polynomials, thus the elements are called 'high order'. Elements with small numbers of nodes are referred to as 'low order'. Neumann and Witherspoon (1970,1971) applied the finite element method to a steady state dam seepage problem with greatly improved results by comparison with finite difference solutions. Pinder and Frind (1972) used a deformed two dimensional isoparametric element in approximating the performance of an aquifer in Nova Scotia. They determined that a large number of linear (low order) elements gave results comparable to a smaller number of high order elements. In fact, high order elements were seen to be more accurate early in the simulation, but the lower order elements were more accurate in the later stages. This result was important because the choice of element and basis function depended on the type of problem to be solved. If the transient state solution was the more important result, then a high density of low order elements was preferred over a small number of high order elements. Since most aquifers rarely come to steady state, a large number of low order elements was preferred, a result also noted by Zienkiewicz (1971) for stress problems in thin plates.

France (1974) was one of the first to apply the finite element method to a non-steady state groundwater problem. He solved a seepage problem where a stream was adjacent to an

unconfined aquifer. The system was not modeled as truly time variant, but was approximated by a series of steady state solutions separated by small time steps, the water level in the stream being gradually increased at each time step. His procedure required iterations to determine the free surface location. The mesh geometry was changed at each time step. The method of simulating the moving interface by a series of steady state solutions became a standard in groundwater modeling, particularly for seepage problems where the fluid level in the aquifer is determined by a slowly moving constant head boundary (Merva and Fausey, 1984). Unfortunately, the method is not suitable for true time variant studies because any local disturbances are immediately smoothed out by the numerical procedure.

Gupta and Tanji (1976) successfully simulated a multi-layered aquifer in California using low order three dimensional deformable isoparametric elements similar to those of Pinder and Frind (1972). The aquifer simulated was three layered with confining zones between layers. A further complicating factor was the existence of a fault which passed through the area. Cunningham and Sinclair (1979) used a two dimensional rectangular finite element mesh to model a coupled groundwater and surface water system in northern Nevada. They solved the two dimensional transient saturated groundwater equation and the one dimensional gradually varied unsteady

open channel flow equations simultaneously in order to represent the truly coupled system. The difficulty with this approach is that the Saint-Venant equations for stream flow must be solved for a time step much shorter than that of the groundwater equation. Thus, an iterative procedure results in which the surface water equation is solved for a large number of short time steps, then the groundwater equation is solved for one long time step with the results of the surface water simulation used as boundary conditions. This process was repeated until the same lateral flow between the stream and the groundwater was estimated from both the stream and groundwater models. Even given the complexity of the solution procedure, the authors had doubts as to the improvement of the model over the less esoteric method of treating the surface water conditions as being constant over each groundwater step. This is a significant result because it indicated that the lack of accurate data on aquifer permeabilities and storage coefficients outweighs the improved accuracy of a more sophisticated solution procedure.

Guvanasen and Volker (1980) had used two dimensional deformable isoparametric elements to model seepage surfaces in sand island studies with considerable success. They compared the backward Euler and Crank-Nicholson time stepping schemes and concluded that the backward Euler scheme was superior because sufficient accuracy was achieved without introducing

numerical 'noise' in the solution.

More recently, Bettess and Bettess (1983) used deformable isoparametric elements to model free surface flows in open channels. Different methodologies for deforming the mesh were discussed. The method used in the final free surface model was that of a simple stretching or compression of the elements in the vertical direction. At each iteration of the free surface the position of the nodes at the free surface was set to the potential function values at that point. The nodes beneath the surface were moved to a position proportional to that of the surface value according to the density of the nodes in the vertical. The nodes at the base of the flow did not move throughout the simulation.

Other Groundwater Models

There are many groundwater models available which use the finite difference method. The two dimensional model of Trescott et al. (1976) has been used extensively by hydrologists since its introduction. The model was written in FORTRAN '66 and all data are stored in memory at runtime. The model was extensively modified for various specialized situations, and so McDonald and Harbaugh (1983) published a revised and reworked version which could simulate flow in two or three dimensions and contained many refinements over the original model. Both the model of Trescott et al. (1976) and the model of McDonald and Harbaugh (1983) do not solve the

non-linear unconfined equation correctly because the position of the free surface is not calculated. Rather, a procedure whereby the specific storage is updated for each step is implemented. The models described in this thesis represent a significant advance in the state of the art over the finite difference models.

The three dimensional model has a somewhat modular structure. Unfortunately, it is difficult to write a truly modular program in FORTRAN because, as one of the first programming languages, FORTRAN was designed specifically for numerical work (FORmula TRANslator). FORTRAN programs tend to be difficult to understand because of a restricted variable naming convention, a lack of data structures and a reliance on the GOTO statement for the control of program flow (although enhancements to the original language have improved flow control instructions). Thus, a truly modular program should be based on one of the newer block structured languages such as Pascal, Modula II or ADA which have a rich instruction set for program control combined with data structures.

EQUATION OF GROUNDWATER FLOW

The parabolic partial differential equation for the flow of an inviscid fluid in a saturated porous medium may be written thus:

$$S_s u_t = \nabla . k \nabla u + J \quad \text{in } Q \tag{1}$$

with boundary conditions:

$u = g1$ on T1

$u_n = g2$ on T2

such that T1 + T2 = complete boundary of Q

and initial conditions: $u = g0$ on D where D = (Q+T1+T2)

where u = Total fluid potential (position + pressure) at a point in the saturated porous medium (L)

u_t = partial derivative of u with respect to time.

Q = domain of the saturated portion of the porous medium.

T1 = Dirichlet portion of the boundary of Q, corresponding to the fixed potential portion of the boundary of the saturated domain. A fixed water level lake may cause this type of boundary condition.

T2 = Neumann portion of the boundary of Q, corresponding to a fixed slope on the solution surface. A boundary with a known rate of flow, i.e. infiltration or regional groundwater flow would cause this type of boundary condition.

k = Darcy saturated hydraulic conductivity ((L/t)) which could vary in each cartesian direction. It is therefore a tensor of permeabilities.

S_s = Specific storage of the porous medium (1/L). This parameter is defined as Sc/b where Sc is a constant dimensionless storage coefficient for a given aquifer material,

and 'b' is the depth of flow which is constant for confined aquifers, but is the saturated thickness (a function of u) for an unconfined aquifer. Thus, Equation 1 is non-linear in u for the unconfined case.

J = A term representing the sources and sinks in the domain (L/t). Source terms may include pumping wells or streams in the domain.

n = directional vector normal to the boundary of Q.

u_n = normal derivative of u with respect to n.

Finite Element Formulation

The method of weighted residuals

The method of weighted residuals is based on the principle that u(x,y,z,t), the solution of Equation 1, can be approximated by a finite sum of N 'basis' or 'test' functions $\phi_j(x,y,z)$ multiplied by a set of time-varying constants, $c_j(t)$. That is:

$$u(x,y,z,t) \sim U(x,y,z,t) = \sum_{j=1}^{N} c_j(t)\,\phi_j(x,y,z) \qquad (2)$$

We will assume that each basis function has an identifying node in the domain, so N is also the total number of nodes. Once the basis functions have been selected, a method for determining the coefficients $c_j(t)$ for $1<j<N$ must be designed. First write Equation 1 in operator form:

$$L(u) = S_s u_t - \nabla.k\nabla u - J = 0 \qquad (3)$$

The method of weighted residuals requires the choice of a set of weighting functions $W_j(x,y,z)$ in addition to the basis functions $\phi_j(x,y,z)$. The coefficients $c_j(t)$ are defined by the requirement that the residual L(U), generated when the approximation of Equation 2 is substituted into Equation 3 be orthogonal to each of the weighting functions, that is

$$\int_D W_j(x,y,z)\, L(U)\, dx\, dy\, dz\, dt = 0, \quad j = 1..N \tag{4}$$

where U, the Galerkin approximation to u, is the sum:

$$U = \sum_{I+Dir+Neum} c_j(t)\, \phi_j(x,y,z)$$

and j runs over the three indexed set of nodes:

I = Interior nodes
Dir = Dirichlet nodes
Neum = Neumann nodes

and N, the total number of nodes is the sum of the Interior nodes, the Dirichlet nodes and the Neumann nodes.

The c_j for the Dirichlet nodes are determined by the Dirichlet boundary conditions and the c_j for the Interior and Neumann nodes are determined by the Method of Weighted Residuals. Thus, Equation 4 reduces to a system of N equations for the N unknown c_j's. In the Galerkin method, the weighting functions are chosen to be identical to the basis functions, ie $W_j(x,y,z) = \phi_j(x,y,z)$. If the functions $W_j(x,y,z)$ and $\phi_j(x,y,z)$ are also chosen such that they are non-vanishing only in a small portion of the domain, then the

finite element method results. Since $W_j(x,y,z)$ and $\phi_j(x,y,z)$ are identical, $\phi_j(x,y,z)$ may be substituted for $W_j(x,y,z)$ in Equation 4 to obtain Equation 5.

$$\int_D \phi_j(x,y,z)\, L(U)\, dx\, dy\, dz\, dt = 0, \quad j = 1..N \tag{5}$$

Conversion to Solvable Form

Now consider Equation 5 and how it can be transformed into a form suitable for numerical solution. Substituting for L(U) from Equation 3 into Equation 5, we obtain:

$$\int_D (S_s U_t - \nabla.k\nabla U) - J)\phi_j\, dx\, dy\, dz\, dt = 0, \quad j = 1..N \tag{6}$$

It is convenient to define an inner (or dot) product of the functions f and g both in its continuous form and discrete approximation as:

$$\langle f,g \rangle = \int_D f\, g\, dx\, dy\, dz = \sum_{i=1}^{M} w_i f_i g_i$$

Where M is the number of quadrature points used in the numerical approximation to the dot product and w is a weight associated with each quadrature point.

Applying the divergence theorem of Gauss to Equation 6, we obtain:

$$\langle S_s U_t, \phi_j \rangle + \langle k\nabla U, \nabla\phi_j \rangle - \langle J, \phi_j \rangle - \int_{T2} U_n\, k\, \phi_j\, dT2 = 0$$
$$j = 1..N \tag{7}$$

where U_n is the partial derivative of U normal to T2.

Equation 7 is a semi-discrete approximation because the equation has not been diacretized in time. The time derivative can be discretized by a backward Euler approximation, an unconditionally stable implicit finite difference scheme. Implementing the backward Euler temporal approximation, and substituting Equation 2 into Equation 7, Equation 8 is obtained. Since the application of the divergence theorem results in the surface integral of the normal derivative of U on the boundary T2, g2 may be substituted into the last term on the right hand side of Equation 8 for U_n since U is the numerical approximation to u. This is how the Neumann boundary conditions are incorporated into the solution.

$$\sum_{j=1}^{N} S_s \frac{c_j^{n+1} - c_j^{n}}{\Delta t} \langle \phi_i, \phi_j \rangle + \sum_{j=1}^{N} c_j^{n+1} \langle k\nabla\phi_i, \nabla\phi_j \rangle$$

$$= \langle J, \phi_j \rangle + \int_{T2} k\, \phi_j\, g2\, dT2, \quad j = 1..N \qquad (8)$$

Superscripts denote time steps and subscripts denote spatial coordinates. Multiplying both sides of Equation 8 by Δt and rearranging yields:

$$\sum_{j=1}^{N} c_j^{n+1} \left(S_s \langle \phi_i, \phi_j \rangle + \Delta t \langle k\nabla\phi_i, \nabla\phi_j \rangle \right)$$

$$= \sum_{j=1}^{N} c_j^{n} S_s \langle \phi_i, \phi_j \rangle + \Delta t \langle J, \phi_j \rangle + \Delta t \int_{T2} k\, \phi_j\, g2\, dT2, \quad j = 1..N \qquad (9)$$

Equation 9 can be written in matrix form thus:

$$Ab = f \tag{10}$$

where $A_{ij} = \sum_{j=1}^{N} (S_s\langle\phi_i,\phi_j\rangle + \Delta t\langle k\nabla\phi_i,\nabla\phi_j\rangle)$

$$f_j = \sum_{j=1}^{N} c_j^n S_s\langle\phi_i,\phi_j\rangle + \Delta t\langle J,\phi_j\rangle + \Delta t \int_{T2} k\,\phi_j\, g2\, dT2$$

and $b_j = c_j^{n+1}$

Initial values for the c_j's are required because the c values at time zero are required to assemble the right hand side of Equation 10 to obtain the solution at time step 1.

Basis Functions and Finite Elements

For the solution of Equation 10 in three spatial dimensions, a hexahedral element was chosen with nodes only at the corners, hence a 'tri-linear' basis function results. This is a three-dimensional variation of the linear 'hat' or 'chapeau' basis function commonly used in one-dimensional finite element work. The element used in the two-dimensional version had four nodes and a 'bi-linear' basis function analagous to the three-dimensional form.

The accuracy and efficiency of the Galerkin method is generally dependent on the choice of basis functions. The linear basis was chosen for the groundwater problem because it offered suitable accuracy with a minimum of computational effort. The basis functions are also usually chosen so that

they can satisfy the Dirichlet boundary conditions exactly. By choosing the cj's on the boundary to be the value of the Dirichlet boundary condition, the Dirichlet boundary condition can be satisfied by the linear basis function.

Triangular elements were popular before the discovery of the isoparametric element because they could handle complicated boundary geometries easily. The use of isoparametric elements allows different types of elements to be effective in approximating boundary geometries (including free surfaces), so a hexahedral isoparametric element was chosen for this research. The concept of the isoparametric transformation is that all elements in the 'global' or 'real' coordinate system can be mapped or transformed into a 'local' coordinate system by the very same basis function which defines the element. Thus, instead of performing all the integrations of Equation 5 on an element-by-element basis, each element is mapped into the local coordinate system for integration. The linear hexahedral isoparametric element is shown in Figure 1.

A linear element was chosen mainly for simplicity and ease of use. Though it would have been more complete to allow the user to choose from a range of available elements, it was not practicable in the context of this model to include such a feature. If the region of flow in question has steep

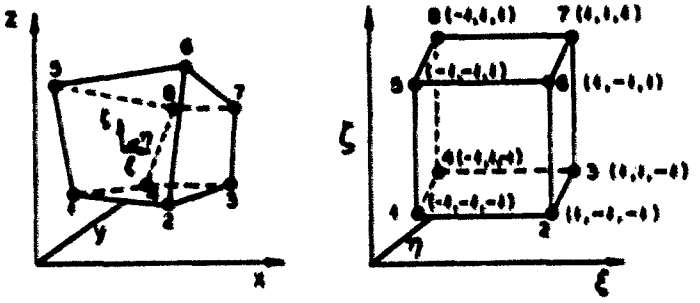

Figure 1. Isoparametric hexahedral elements in global (x,y,z) and local (ξ,η,ζ) coordinates (after Lapidus and Pinder, 1982)

gradients or the user requires detailed results, then a high density of elements should be used.

Numerical Integration

Zienkiewicz (1971) recommended second order Gaussian quadrature for linear isoparametric elements, with third order being the maximum suggested. This order of quadrature resulted in four and eight quadrature points in the two and three dimensional models, respectively. The implementation of the isoparametric element formulation is a relatively straightforward process, the details of which may be found in Ciarlet (1978), Bathe and Wilson (1976) and Zienkiewicz (1971).

Maximum Time Step

Guvanasen and Volker (1980) used a backward Euler temporal procedure to model free surface flows in sand island

seepage studies. They found from numerical experiments that the maximum allowable time step was:

$$delt < (4.0\ Ss\ dx)/(k\ b) \qquad (11)$$

where: dx = the smallest dimension of an element in the mesh.
b = the saturated thickness for an unconfined aquifer and the aquifer thickness for a confined aquifer.

Equation 11 gives time steps in the order of a few hours for practical systems. If conditions are close to steady state then this can be extended without significant errors on large scale aquifers.

Solution of the System of Equations

The left hand side matrix (A) of Equation 10 is a non-singular positive-definite diagonal symmetrical matrix (Gary, 1975). Cholesky factorization is ideally suited to the solution of such a system of equations. The matrix may also be stored in 'profile' form, with only part of the matrix actually present. Only the elements from the first non-zero element on a row to the diagonal are stored. The integer position of the diagonal elements are also required. Thus, a vector storage form results which is much more efficient than storing the entire matrix. Jennings (1977) gives an algorithm for Cholesky factorization and subsequent solution. The factored matrix uses the same memory space as the original form and requires few temporary storage locations. The main advantage of the Cholesky method is that numerical errors are minimized because most operations are performed on numbers of

similar order. A further advantage of the Cholesky method is that for systems in which the mesh does not change (a confined aquifer), the factorization need only be performed once.

Solution for an Unconfined Aquifer

Equation 1 is a linear equation for a confined aquifer because the specific storage is a constant. Flow with a free surface is non-linear because the value of the specific storage depends on the saturated thickness of the aquifer. Thus, Equation 1 must be solved in an iterative fashion. There are basically two mesh geometry schemes by which the free surface equation may be solved:

1. Fix the element mesh and vary the element properties so as to model the position of the free surface. This approach is applicable to a saturated-unsaturated model as used by Desai and Li (1982) in earth dam problems. The disadvantage of this approach for this type of model is that the nodes which fall outside the saturated domain are lost as far as relevance to the saturated problem is concerned, and therefore represents a loss of resolution in the vertical. The second disadvantage is that the location of the free surface must be approximated by a piecewise interface which passes along fixed element boundaries, and is therefore not well defined unless a very large number of elements are used.

2. Extend the finite element mesh from the lower confining surface to the free surface and, as iterations are performed, move the position of the free surface (Figure 2). This approach is more favorable for the saturated model because it avoids the two disadvantages of method 1. The position of the free surface must still be found by iteration.

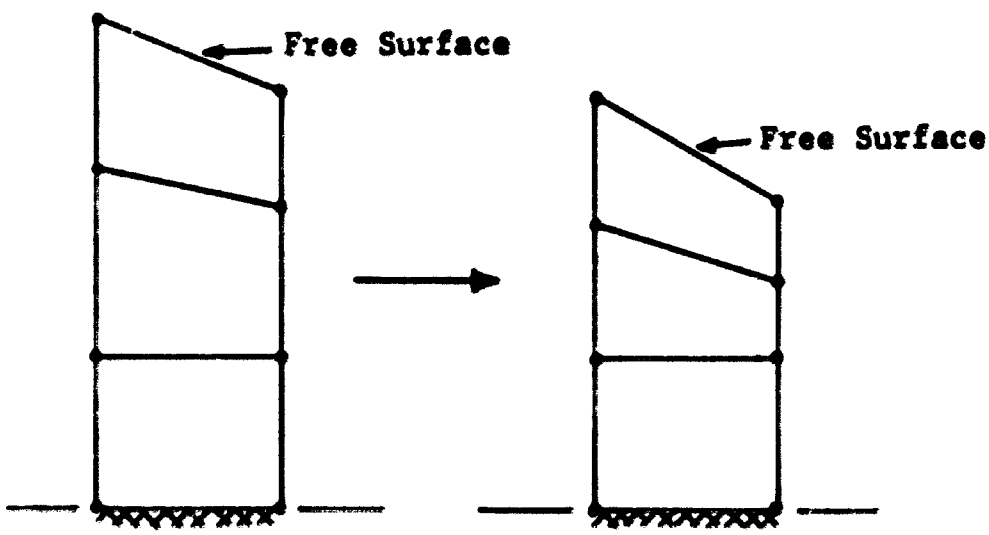

Figure 2. Deformation of finite element mesh with change in the free surface

The second method was therefore chosen for this problem. The method of free surface iteration must also be chosen. There are also two main options available for the procedure to estimate the location of the free surface.

1. Use elements which have two variables at each node, namely the function value itself, and the velocity of the

phreatic surface normal to the free surface. Thus, the position of the free surface for the next time step may be estimated by a simple multiplication of the estimated velocity by the time step involved. The process is repeated until convergence is achieved. This is a Newton-Raphson method of iteration to find the final position of the free surface. The disadvantages of this approach are twofold. First, the number of unknowns in the system is doubled by using two variables at each node, and therefore reduces the allowable number of nodes in a small computer system by almost one-half. It should also be noted that this degree of sophistication is wasted in a simulation of a confined aquifer since the mesh does not move. Secondly, the normal direction to the free surface must be estimated. To this end, most researchers to date have fitted a cubic spline approximation to the surface, and then found the normal to the resulting polynomial to achieve the normal direction. This is a reasonable approach in two dimensions (horizontal and vertical), but would be a very large and time-consuming approach for three dimensions, particularly on a small computer.

2. The use of simple Lagrangian elements (one variable per node) with a "relaxation" scheme to determine the free surface position is also possible. This approach, while

not as esoteric as the first method, is less demanding on memory which is of prime importance on small computers. The method proceeds as follows: The current solution (assumed to be such that the mesh matches the free surface) is stored in a temporary array. The system is then solved with the mesh held fixed, and an interim solution obtained. This interim solution is then compared with the position of the mesh to determine if the free surface potential corresponds to the position. If the difference between the two is sufficiently large, the mesh is moved to the interim solution position and the procedure is repeated until the position of the free surface is approximated to within a certain tolerance. The scheme converges to the correct free surface position for all initial conditions except one case. Normally, the scheme works for a withdrawal situation because the position of the interim solution is always a conservative estimate of the actual free surface (i.e., it always has a greater depth of flow). The only way for the method to fail to converge is if the user inputs a mesh which has an extremely small saturated thickness for the amount of withdrawal involved. In this case, (analogous to a confined aquifer with high withdrawal rates), the free surface may not rise in the first approximation because the aquifer cannot possibly transport enough water. If

the depth of flow is small, then extremely large drawdowns will result, thereby dewatering the system and causing the failure of the program because the elements will have zero volume.

If water is pumped into the aquifer then the method will also converge because the mesh will increase in depth at each iteration. Since the method stability depends on the stability of the backward Euler numerical scheme employed, and on no other factors, then there are no further restrictions on the allowable time step other than those of the backward Euler scheme. Table 1 shows the convergence of the method for a simple example. Convergence is usually achieved in three or four iterations, even for the most stringent conditions. The data for Table 1 were collected from a very demanding problem in which the free surface moved a great deal during each time step.

Table 1. Convergence of the Free Surface Iterative Scheme

Iteration number	Maximum error between the Mesh location and the free surface solution surface (m)
1	23.2029
2	2.5405
3	0.0505
4	0.0007

PRECIPITATION TRANSPORT MODEL

Rainfall enters the groundwater (saturated) zone by two mechanisms. Infiltration determines the amount of water which passes through the first few centimeters of the soil profile. From there to the phreatic surface, seepage transports the infiltrated water to the saturated zone. In addition to the transport process, evapotranspiration and moisture redistribution must also be taken into account since the actual amount of infiltrated water which reaches the saturated zone may be very small. The result from the infiltration model described in the following chapter is introduced into the groundwater model as a Neumann boundary condition at the free surface in Equation 10.

Infiltration Model

It is particularly important to have a good model of infiltration in a continuous simulation groundwater model because infiltration plays such a large role in the recharge of groundwater. The correct simulation of the infiltration process has held the attention of many researchers throughout the years, and it seems now that the analytical tools exist with which the process can be modeled with sufficient accuracy. Unfortunately, it is not a simple task to measure the required parameters for field application, much less cope with the problems of anisotropy and inhomogeneity in the soil

profile. For a continuous simulation model, an infiltration model based on storage in the soil is preferred over a single-event model because soil moisture is retained between rainfall events. An infiltration equation which meets this requirement is the Green-Ampt equation (Green and Ampt, 1911) which has enjoyed considerable attention in recent years. The basis of the Green-Ampt model is that water in the soil pores is acted upon by the forces of gravity and capillary suction. Thus, the only force which changes with time is the capillary suction force, a function of the degree of saturation of the soil. The Green-Ampt equation is written as follows:

$$f = Ks\ (1 + Su.IMD/F) \qquad (12)$$

where f = infiltration rate (mm/s)

Ks = Green-Ampt saturated hydraulic conductivity (mm/s)

Su = average capillary suction at the wetting front (mm)

IMD = initial moisture deficit for this event (mm/mm)

F = cumulative infiltration volume for this event (mm)

Therefore, the infiltration rate is not an explicit function of time, but a function of the total infiltration volume which has preceded that time. The parameters involved in the equation have some physical significance (Morel-Seytoux et al., 1974) which is in contrast to most other models.

Green and Ampts' original equation was for the case of excess surface water at all times. Mein and Larson (1973) showed how the model could be applied to a steady rainfall. Chu (1978) adapted it to an unsteady rainfall. The Mein-Larson model is a two stage model. The first step predicts the volume of water which will infiltrate before surface saturation. If this volume is exceeded then the infiltration amount is predicted by the Green-Ampt equation. If the volume of infiltration is not sufficient to saturate the surface then the infiltration rate is equal to the rainfall rate. The value of F in the Green-Ampt equation is used as the total infiltration during the rainfall event. Wilson et al. (1982) and others have further refined the Mein-Larson model to account for the effects of entrapped air and air resistance on the time to surface saturation. Unfortunately, work on the effect of air entrapment has not progressed to the point where satisfactory data are published on how to apply the corrections to field work. For the purposes of this work, the Mein-Larson Model will be used without correction for air entrapment.

The Storm Water Management Model SWMM (Huber et al., 1982) uses the Mein-Larson model with modifications for redistribution of infiltration and estimates of the time since the last significant rainfall event. Subsurface drainage and moisture redistribution between rainfall events decrease the

moisture content in the upper soil layers and increase the infiltration capacity of the soil. A simple empirical routine was presented to determine a depletion factor to be applied to the soil moisture deficit (IMD) and total infiltration (F) in between rainfall events.

$$\text{Depletion factor} = 0.0672\ Ks^{.5} \quad \text{(mm/hour)} \tag{13}$$

Equation 13 assumes that the amount of redistribution is dependent on the saturated hydraulic conductivity of the soil. If Ks is large (sands, gravels), then there would be a large amount of redistribution. If Ks is small (clays), then redistribution would take place much more slowly because the soil would not drain as quickly. The estimate of the time between significant rainfall events was also presented as being dependent on the saturated hydraulic conductivity of the soil for the same reasons as the depletion factor. The equation presented by Huber et al. (1982) for the time between significant rainfall events was:

$$T = 0.06/\text{Depletion Factor} \tag{14}$$

where T = time between significant rainfall events (hours)

At times beyond the value estimated given by Equation 14, further rainfall was considered as an independent event and soil moisture deficits were set to initial values.

Prediction of Green-Ampt Parameters

Whilst many papers have been published on the advantages and disadvantages of the Green-Ampt Model on a theoretical level, there still remains the problem of estimating parameters without extensive field and laboratory work. A few researchers have tackled the problem. The three parameters required for the Green-Ampt model are the Green-Ampt saturated hydraulic conductivity (Ks), the wetting front capillary suction (Su), and the initial moisture deficit (IMD). Of these three, the Green-Ampt saturated hydraulic conductivity and moisture deficit are relatively straightforward to measure. Brakensiek and Rawls (1982) reported that the Green-Ampt saturated hydraulic conductivity (Ks) should be taken as one-half of the saturated conductivity. The initial moisture deficit (IMD) is the fraction difference between soil porosity and the actual moisture content and may therefore be estimated directly from soil tests or from a review of literature. The most difficult parameter to measure is the capillary suction parameter (Su). Published values of Su are extremely variable and do not seem to follow any particular pattern. Fortunately the performance of the Mein-Larson model is not very sensitive to the value of Su (Huber et al., 1982).

Rawls and Brakensiek (1983a) estimated Green-Ampt parameters from an extensive soil survey. They concluded that a reasonable estimate of the parameters could be made based on

soil texture class. While there is a general trend of the parameters according to soil class, the variation within each soil class was very large. More recently, Rawls and Brakensiek (1983b) described a procedure which was based entirely on soil classification and attempted to account for the effects of crusting, tillage and organic content. The SWMM model (Huber et al., 1982) lists capillary suction values and initial moisture deficits from a survey of various researchers. The data shown in Tables 2, 3, and 4 are given only as guides. New material is published frequently about the Green-Ampt parameters so any new information should be used to supplant the data given below. The values of saturated hydraulic conductivity listed in Table 2 are unmodified for the Green-Ampt model, so should be divided by two if used as Ks, the Green-Ampt saturated hydraulic conductivity. Such is the variability of soils even within the same texture class that the user should be prepared to adjust the parameters for best results.

Table 2. Range of saturated hydraulic conductivity values (after Bouwer, 1978)

Soil Texture	K (m/day)
Clays (surface)	0.01-0.2
Loams	0.1-1
Fine Sand	1-5
Medium Sand	5-20
Coarse Sand	20-100
Gravel	100-1000
Sand and Gravel Mixes	5-100
Till	0.001-0.1

Table 3. Typical Green-Ampt IMD values (after Huber et al., 1982)

Soil Texture	Typical IMD at Wilting point
Sand	0.34
Sandy Loam	0.33
Silt Loam	0.32
Loam	0.31
Sandy Clay Loam	0.26
Clay Loam	0.24
Clay	0.21

Table 4. Typical values of Su (after Huber et al., 1982)

Soil Texture	Su (mm)
Sand	102
Sandy Loam	203
Silt Loam	305
Loam	203
Clay Loam	254
Clay	178

Sub-Surface Model

The transport of water through the unsaturated zone is a complicated process which has prompted the creation of complex numerical simulations in its own right. For the purposes of this groundwater model, a less complicated solution was sought which would model the process without resorting to a computationally intensive algorithm. Just as the Green-Ampt infiltration equation is based on the concept of soil-moisture storage, it seemed reasonable to model the transport process

as storage-dominated. Thus, the soil between the upper layers and the phreatic surface was modeled as a storage tank with an outflow which was controlled by an orifice. Flow passes into the tank from the infiltration model, and is released as a function of the amount of storage in the tank. A schematic of the storage-based transport model is illustrated in Figure 3.

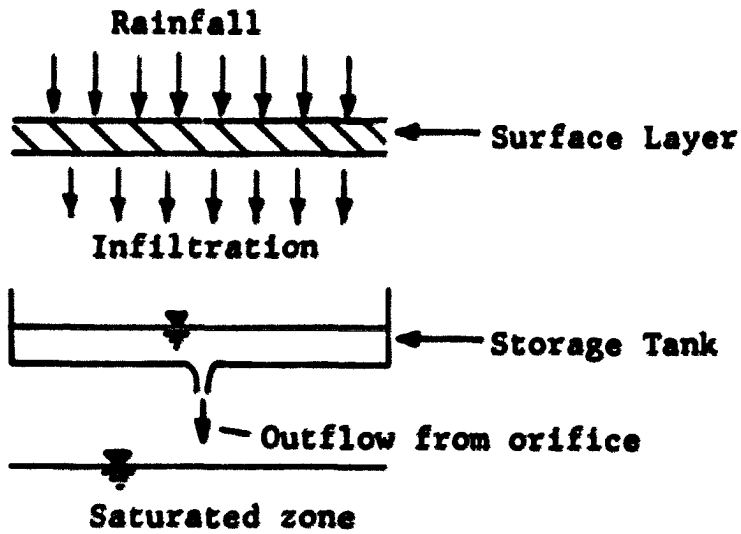

Figure 3. Infiltration - Storage unsaturated zone model

The equation describing flow through an orifice is written thus:

$$V = C\,(2gh)^{0.5} \qquad (15)$$

where V = outflow velocity (mm/s)
g = gravitational acceleration (mm/s/s)
C = constant for orifice (0)
h = depth of fluid above orifice (mm)

The storage analogy model is therefore a one-parameter model in 'C' similar to a Nash Cascade overland flow model with one tank. The 'C' coefficient determines how fast the infiltrated water reaches the saturated zone. If the value of 'C' is large (100) then all the water infiltrated in that time step will pass into the saturated zone without modification by the soil storage model. The precipitation transport model would then act entirely as the Mein-Larson infiltration model. If the value of 'C' is small (1-10), then water is held in storage and released at a very low rate from the orifice. If 'C' is zero then there is no outflow from the orifice and the soil retains all infiltration. Practical values of 'C' range between 0 and 100. A 'C' of zero could apply to a case where an impermeable layer lies just below the surface, or perhaps when the water table is very deep and thus, evapotranspiration carries the water away before it can reach the saturated zone. A 'C' of 100 could apply to a very shallow water table where all infiltration passes very quickly into the saturated zone. Figure 4 shows the variation in outflow from the soil-storage model for a constant rainfall of 2.2mm/hr for 15 hours with varying 'C' values.

The Green-Ampt parameters for the data of Figure 4 were chosen so that all rainfall infiltrated. This allowed an easy mass balance check to be performed on the system. No evapotranspiration was removed during the test runs.

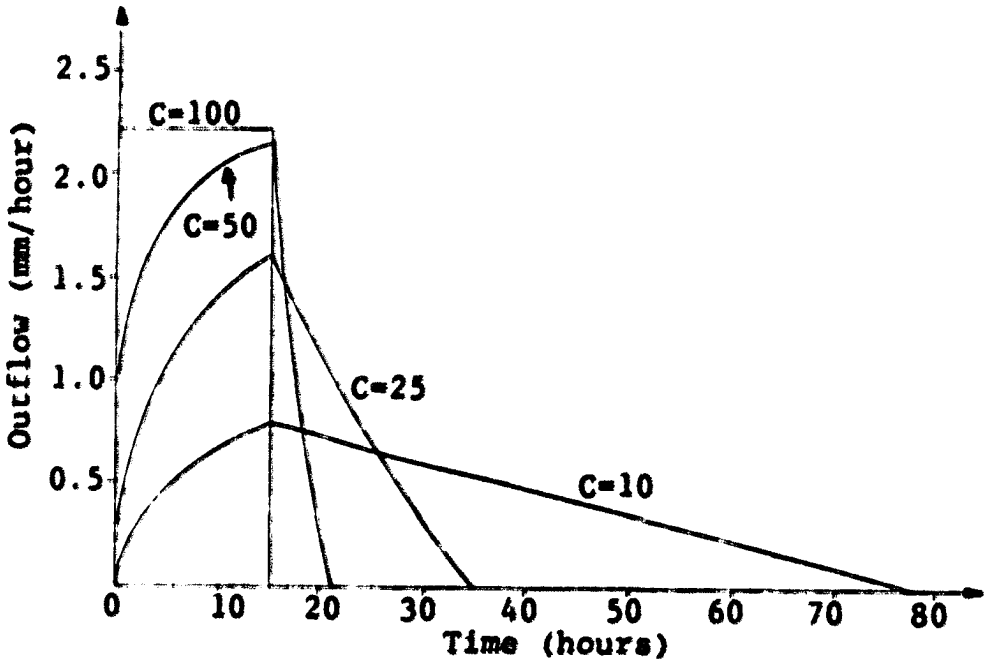

Figure 4. Variation in outflow from the Soil-Storage model with 'C' parameter

Evapotranspiration

Another important process during the passage of rainfall to the saturated zone is that of evapotranspiration. There is no actual calculation of evapotranspiration rates in the model (although it could easily be added later because of the modular nature of the code). The evapotranspiration rate is one of the data inputs provided by the user. The evapotranspiration is entered as a rate in mm/hour for each time step in the model.

Since the model has a two layer scheme for the transport of water to the free surface, evapotranspiration must be removed from both layers. The layer of soil which applies to

the infiltration model is quite thin (on the order of a few centimeters) but all of the surface evaporation comes from this layer. The deeper layer has little evaporation but most of the transpiration since it contains most of the root zone for agricultural crops. It was decided that one-third of the evapotranspiration rate specified would be withdrawn from the upper layer (soil moisture) and two-thirds from the lower layer (storage tank). The percentage of withdrawals from each layer is a constant within the program and would require code modification to change the proportion.

PUMPING WELLS AND STREAMFLOW

The presence of pumping wells or streams in the model area are the two contributions to the source term (J) in Equation 10. Each is modeled in a different way and so will be discussed independently.

Pumping Wells

Pumped or recharge wells in the aquifer are modeled as an averaged withdrawal source over a pumped element. The user specifies that a particular element contains withdrawals (sources), and specifies the volume per unit time which is withdrawn from that element. The radius of the well is not one of the inputs provided. A well is not modeled as a point withdrawal (source) because the model would predict extremely large drawdowns for a true point of withdrawal. In fact, drawdowns would approach infinity as the radius approaches zero.

The simulation of the pumping sources in Equation 10 depends on the way the source term is handled. If the source term rate (J) is considered constant across an element, then the term

$$\langle J, \phi_k \rangle = J.\langle 1, \phi_k \rangle$$
$$= J.(\text{area of element})/3.0$$

because the integral of a basis function over an element is

one-third the area of the base multiplied by the height. But J, the source term strength = Q/(area of element) where Q is the specified volume/unit time of withdrawals. Thus, it follows that:

$\langle J, \phi_k \rangle = Q/3.0$

Thus, for each node on a pumped element, the value Q/3.0 is added to the right hand side of Equation 10. Injection wells are just the negative of pumped wells.

Streams

Streams which penetrate the aquifer may be modeled in two ways. First, as a fixed head Dirichlet boundary condition which corresponds to a perfect recharge boundary with no effect of river bottom sediment. This method of simulation does not allow drawdowns from one side of the river to affect the aquifer on the other side. It assumes an infinite supply of water in the river to recharge the aquifer. If a flowing stream penetrates an aquifer with little or no silt layer, then this condition may be realized. This condition is not applicable when the stream becomes dry, and caution should be shown when dealing with streams that alternate wet and dry conditions.

The second way to model streams is as an element (or cell) which contains a stream as shown in Figure 5. Modeling the stream this way allows movement of water through a bottom

sediment layer which has its own hydraulic conductivity and thickness. Darcy's Law is used across the sediment layer to calculate the rate of flow into or out of the aquifer. Thus, the element which contains the stream has a rate of flow into or out of it and is therefore handled in the same way as a pumped element once the rate of withdrawal or injection has been calculated.

The potentials at the stream nodes are unknowns which change according to the groundwater potential surface. In the case of Figure 5a, the potential in the aquifer is greater than that of the water level in the stream. Water is withdrawn from the aquifer because the potential is decreasing from the aquifer to the stream.

The velocity of flow to or from the aquifer (Vriver) may be written as:

$$Vriver = Kb.(Hriver-Haq)/B \qquad (16)$$

Where Kb = Hydraulic conductivity of river bottom (mm/s)
Hriver = Head in the river (mm)
Haq = Head in the aquifer (mm)
B = thickness of river bottom sediment (mm)

Figure 5b shows the situation when the water table is well below the stream bed. In this case, there is flow through the sediment layer to the aquifer. The rate of flow through the sediment layer is calculated from Darcy's Law with the river stage as the driving force. The bottom of the sediment layer is presumed to be at atmospheric pressure. The

stream flow is input by the user of the model as a volume per unit time for each time step. The stream cross-section is approximated by a trapezoid with uneven side slopes (dimensions input by the user). The river stage is calculated by iteratively solving Manning's equation (Manning's 'n' parameter and longitudinal slope input by the user) for each time step in the model, so the rate of flow to or from the aquifer will change during a simulation. If the groundwater level near the stream drops appreciably during a simulation, then the stream may change from a gaining to a losing condition. The stream flowrate is not altered within the model to account for flow to or from the aquifer, nor are any routing calculations performed on the stream flow during the simulation.

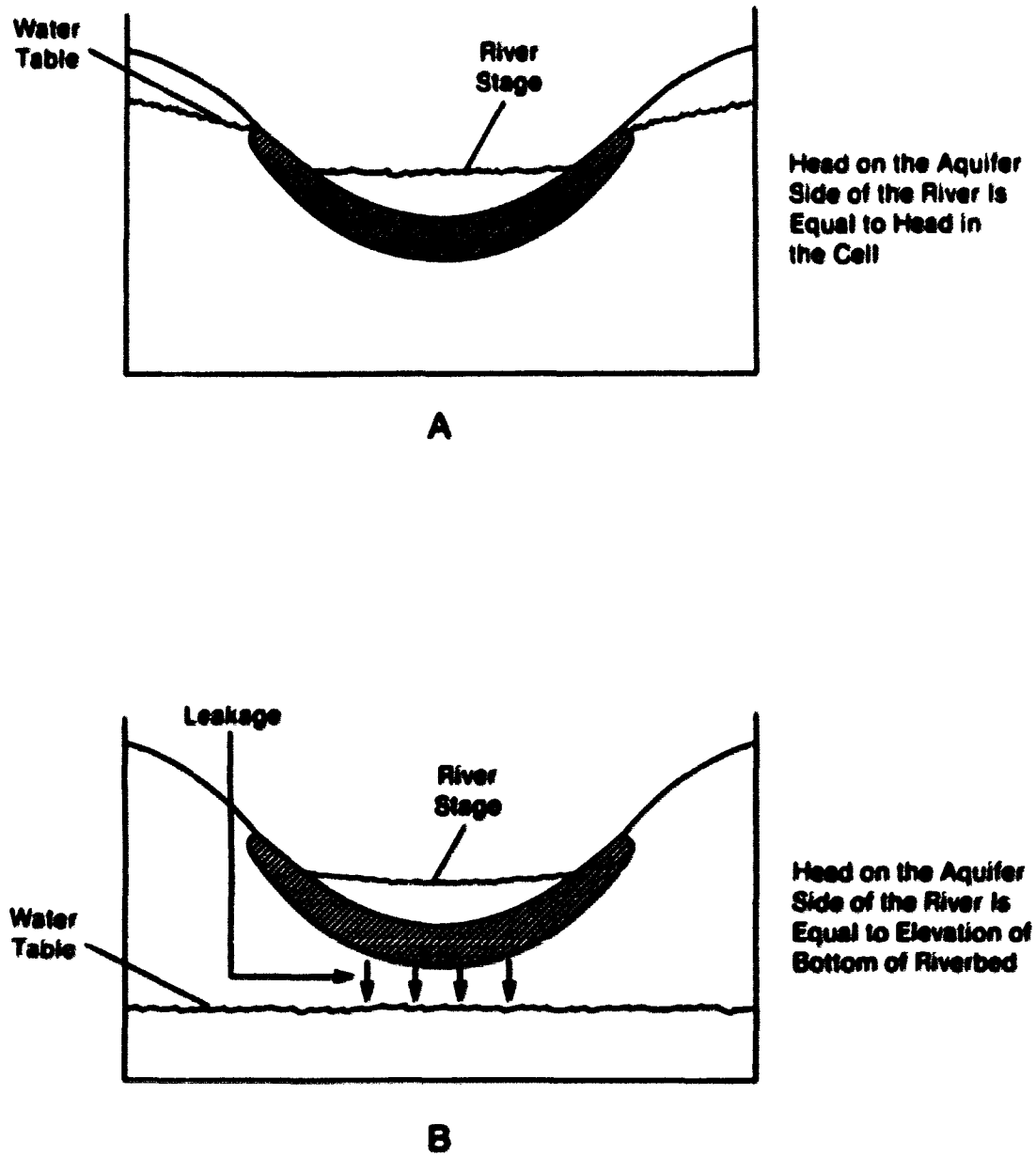

Figure 5. Cross section showing the relationship between head on the aquifer side of the riverbed and head in the stream element (cell). Head in the element is equal to the water-table elevation (after McDonald and Harbaugh, 1983)

MICRO-COMPUTER IMPLEMENTATION

The implementation of the stream-aquifer model on a micro-computer involved a number of design methodologies different from the normal mainframe program implementation. The actual algorithm development was not different for the small machine, but the way in which it was implemented was quite different. On mainframe computers, memory use (sometimes known as core storage) is not an important criterion since large amounts of memory are available. The micro-computer has a strictly limited amount of memory and so measures were taken to ensure that the available memory was used with maximum efficiency. Thus, a disk-based approach was used in which data for the mesh are kept in disk files which the user creates with utility programs. The finite element model reads data for each element from the disk as required, thereby minimizing the memory requirements of the program. In addition, micro-computers come with variable amounts of memory and so program design must allow the program memory requirements to be easily modified. A dynamic memory allocation structure was used to store the large matrix (A) in Equation 10 and program constants were used for all array dimensions. Defining the data structures in this way allows the program memory use to be changed very easily (although it does require recompilation of the code).

Micro-computers have an advantage over the larger machines in the area of user interactiveness. To make the most of this feature, the models used in this thesis were designed to be easy to use and interactive in nature. Most errors in data input can be found before the code is executed which is in sharp contrast to current mainframe models. The programs used to create and modify the disk files were designed to be easy to use and provide meaningful error messages to the user. A graphics program was written to plot the mesh data from disk files which has been found to be extremely useful in detecting data input errors. In addition, a simple contouring program allows the user to immediately see the effects of a particular hydrologic input.

The models were initially implemented in Turbo Pascal on an IBM PC-XT micro-computer with 256 kilobytes of RAM (Read/ write Random Access Memory), a 10 Megabyte hard disk, one 360k floppy disk drive and an 8087 numeric co-processor. The use of the numeric co-processor is mandatory for problems with many elements. The models run under the PC-DOS or MS-DOS operating system and have been tested on a Zenith Z-150 micro-computer with a similar configuration to the IBM PC-XT. The models were written with a view to being easily modifiable if transport to another computer or compiler is necessary.

ANALYTICAL CALIBRATION

The models were calibrated against an analytically solvable problem of transient heat conduction on a unit square.

$$U_t = \nabla \cdot \nabla U + 1 \quad \text{in } \{(x,y): 0<(x,y)<1\} \text{ for } t>0 \tag{17}$$

with boundary conditions:

$$U = 0 \text{ on } (x=1, 0<y<1) \text{ and } (y=1, 0<x<1)$$
$$U_n = 0 \text{ on } (x=0, 0<y<1) \text{ and } (y=0, 0<x<1)$$

and with initial conditions $U(x,y) = 0$ at $t = 0.0$

where: U_t = partial derivative of U with respect to time
U_n = partial derivative of U with respect to the normal to the surface of the domain of U.

A comparison of Equation 17 with the groundwater equation (Equation 1) shows that the mechanisms of heat flow and groundwater flow are identical. Thus, verification of the model performance with a heat flow problem is valid. A two dimensional problem was chosen because a meaningful three dimensional analytically solvable problem could not be found. A twenty-five node two dimensional and a seventy-five node three dimensional model were applied to the problem (Figure 6). The three dimensional mesh was a three layer mesh with symmetry in the vertical to approximate the two dimensional problem. The results of the simulation are presented in Table 5. Both models gave the same results. Reddy (1984) indicated that the steady state should be achieved at time t = 1.0. The

data presented in Table 5 indicated that the transient finite element solution at t = 1.0 displayed a high degree of accuracy when compared to the analytical steady state solution.

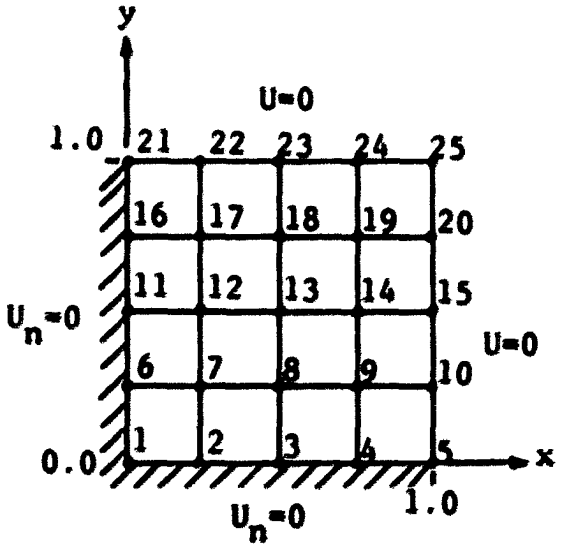

Figure 6. Two dimensional finite element mesh applied to transient heat conduction problem

The maximum error between analytical and numerical solutions was 4.6% which is quite good considering the relative coarseness of the mesh. The time-variant response at node 1 is shown in Figure 7. Application of the models to this example was particularly useful because it indicated that;

a) The correct steady state was achieved. Thus, the source terms are properly handled and the boundary conditions are also correctly implemented.

b) The solution reached the steady state at the correct time, thereby indicating that the time-stepping is also accurate.

c) The time variant solution does not have any serious oscillation problems which would require artificial damping.

Table 5. Comparison of FEM solution with analytical solution to two-dimensional steady state heat conduction problem

Node	Steady State Solution (after Reddy, 1984)	FEM Model at t=1.0	Error
1	0.2947	0.2946	0.0001
2	0.2789	0.2788	0.0001
3	0.2293	0.2295	-0.0002
4	0.1397	0.1399	-0.0002
5	0.0000	0.0000	0.0000
7	0.2642	0.2642	0.0000
8	0.2178	0.2181	-0.0003
9	0.1333	0.1337	-0.0004
10	0.0000	0.0000	0.0000
13	0.1787	0.1819	-0.0032
14	0.1127	0.1135	-0.0008
15	0.0000	0.0000	0.0000
19	0.0711	0.0745	0.0034
20	0.0000	0.0000	0.0000
25	0.0000	0.0000	0.0000

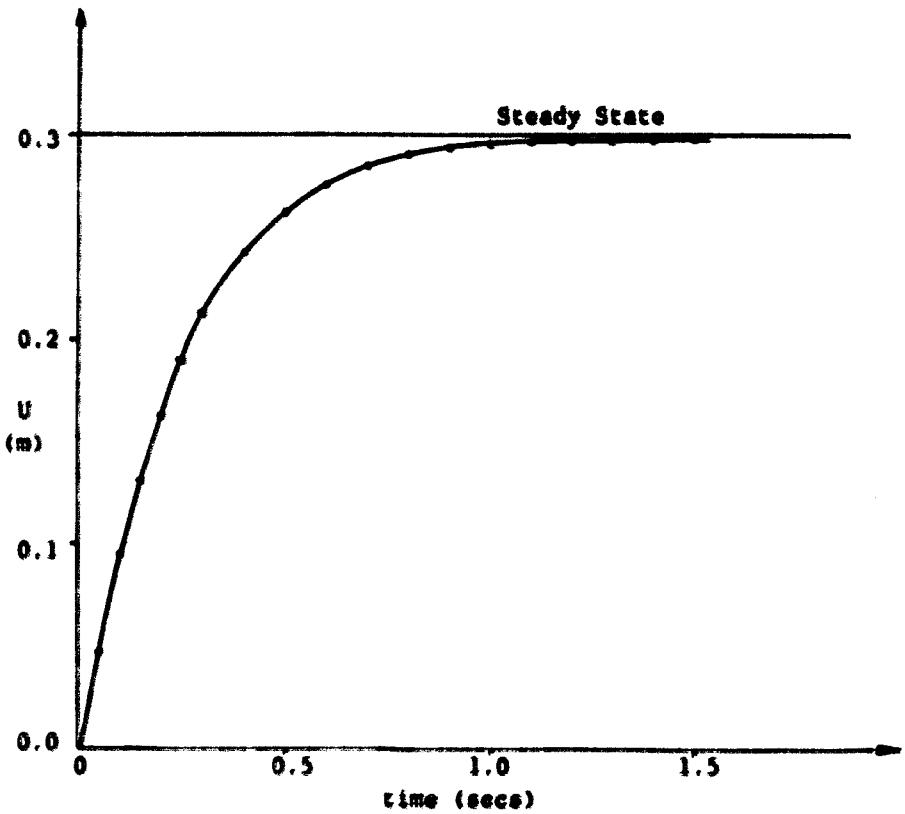

Figure 7. Variation of U with time at node 1 for transient heat conduction problem

TWO DIMENSIONAL MODEL

It was decided to calibrate and verify the two dimensional groundwater model (SAFEM2) to a shallow aquifer system near Ames, Iowa because there were significant stream-aquifer interactions and ample data were available.

Ames Aquifer Area

The City of Ames, Iowa draws its municipal water supplies from a glacially formed buried channel aquifer system. The aquifer consists mainly of saturated sands and gravels overlying bedrock. Figure 8 shows the City of Ames with aquifer boundaries. Delineated glacial drift deposits overlying the aquifer in the downtown area create a weakly confined formation. The aquifer is unconfined to the south and east of the city where recharge comes from the Skunk River and Squaw Creek (Figure 9). Recharge to the confined portion of the aquifer comes mainly from the Skunk River north of 13th Street. The majority of present withdrawals come from the confined area which will be referred to as the Downtown Well Field. A severe drought in 1976 and 1977 with intermittent drought conditions in 1980, 1981 and 1983 caused groundwater levels in the city wells to drop to an unacceptable level. Because of past problems with the aquifer, the City of Ames began studies into alternate water supplies. Preliminary studies of a proposed new well field in the southeast part of

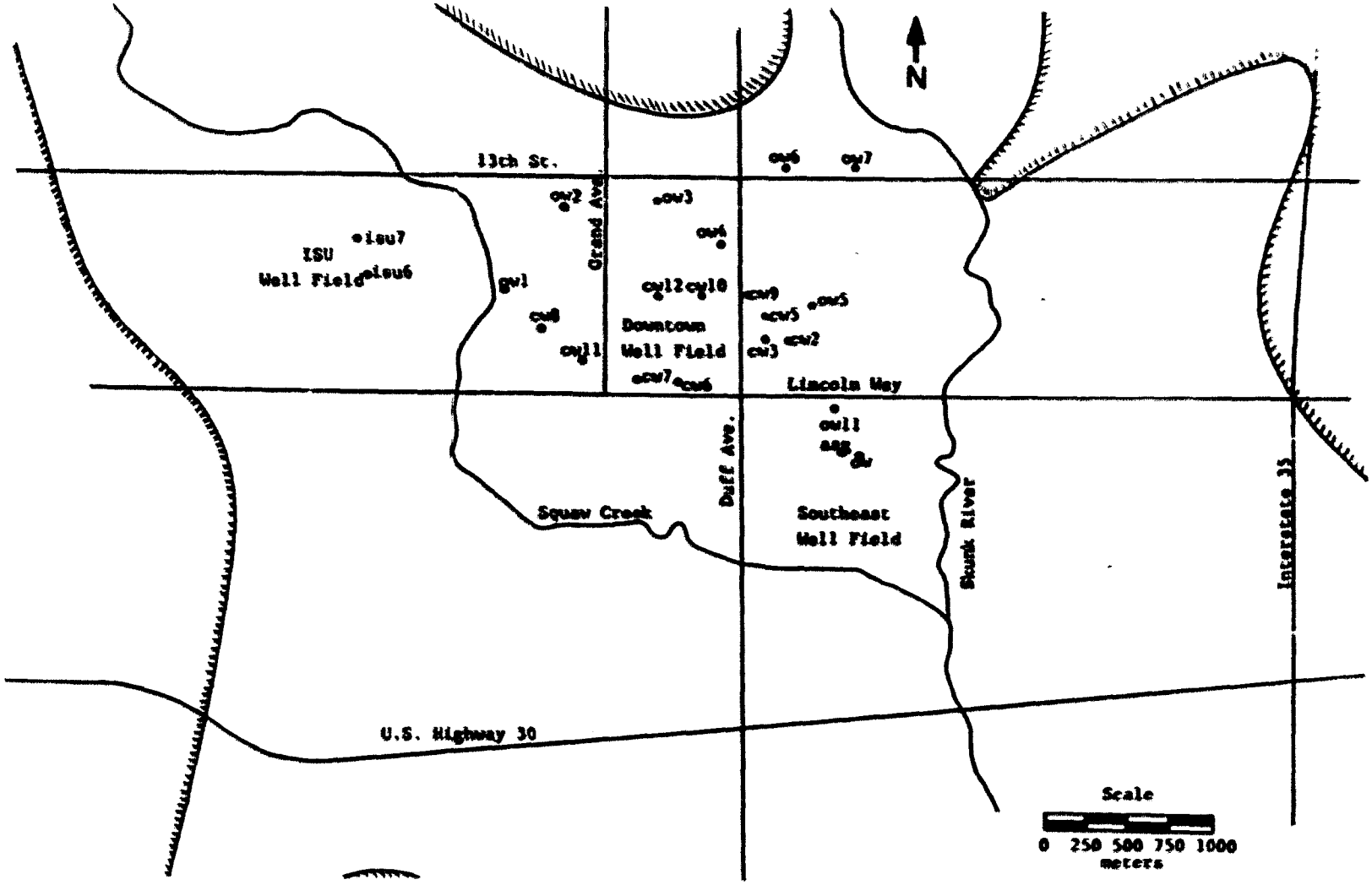

Figure 8. Ames area with observation wells and aquifer boundaries

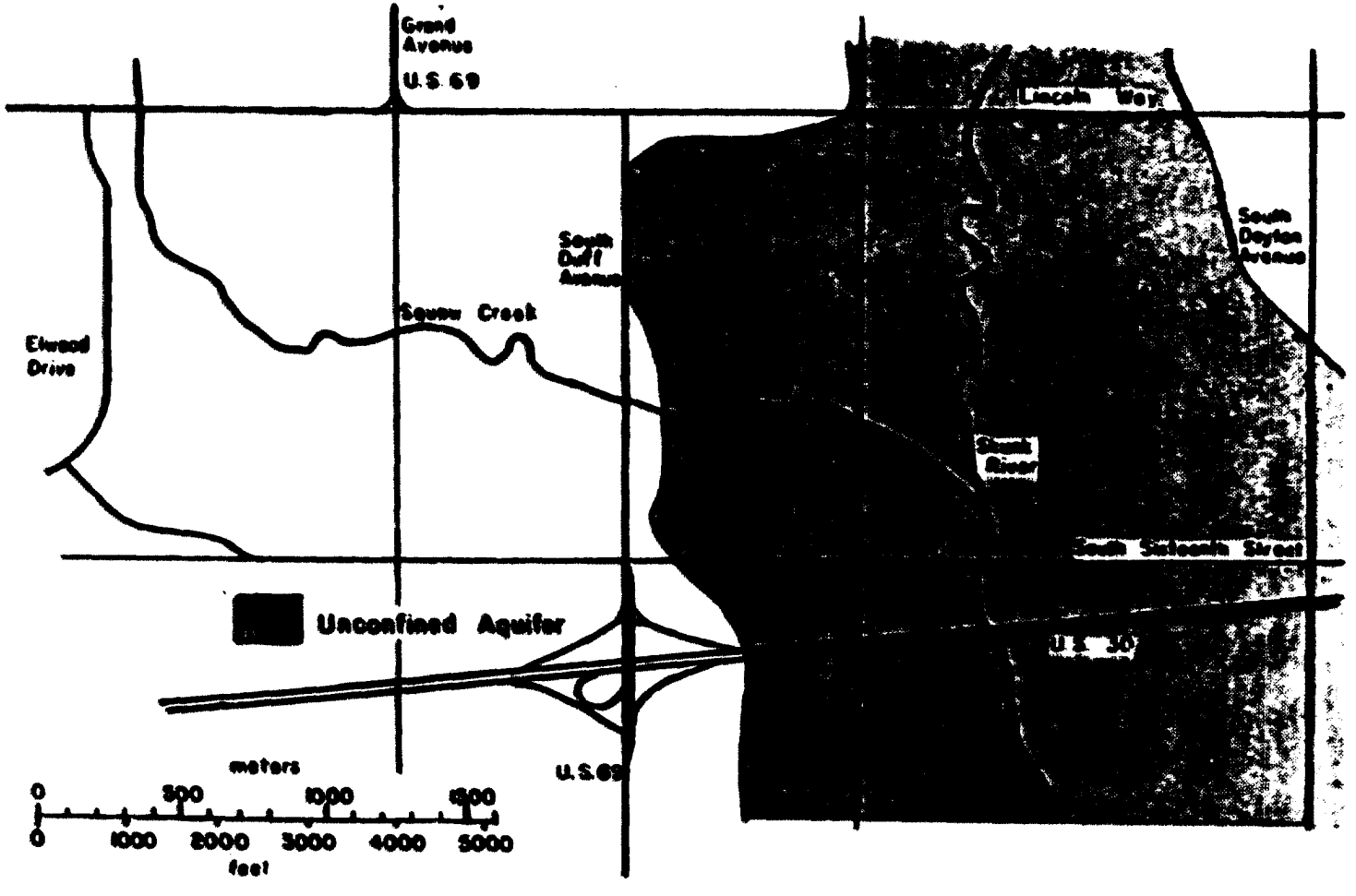

Figure 9. Extent of unconfined portions of the Ames aquifer (after Willie, 1984)

the city (hereinafter referred to as the Southeast Well Field) were conducted by Dougal et al. in 1971, and subsequently refined in a more detailed study by Austin et al. (1984), Willie (1984), and Drustrup (1985).

Aquifer thicknesses (Willie, 1984) in the Southeast Well Field were seen to be larger than that of the Downtown Well Field with very high hydraulic conductivities. Estimated hydraulic conductivities were 2-3mm/s over a thickness of 18-23m (Drustrup, 1985). Thus, the potential for withdrawals from the new system was large. It was considered necessary to simulate long-term pumping from the new well field to determine if drawdowns were acceptable and did not affect other wells in the area.

Calibration to Ames Aquifer Data

A finite element mesh of 378 nodes and 340 elements was applied to the Ames area (Figure 10) with a view to having the most detail in the Southeast Well Field. The size of mesh was close to the maximum which could be stored in the computer used in the simulation. Akhavi (1970) conducted a series of pumping tests to determine aquifer characteristics in the Downtown Well Field. A pumping test in the Southeast Well Field by Austin et al. (1984) was the source of data for the unconfined portion of the aquifer system. Initial aquifer hydraulic conductivities storage coefficients were derived from Drustrup (1985).

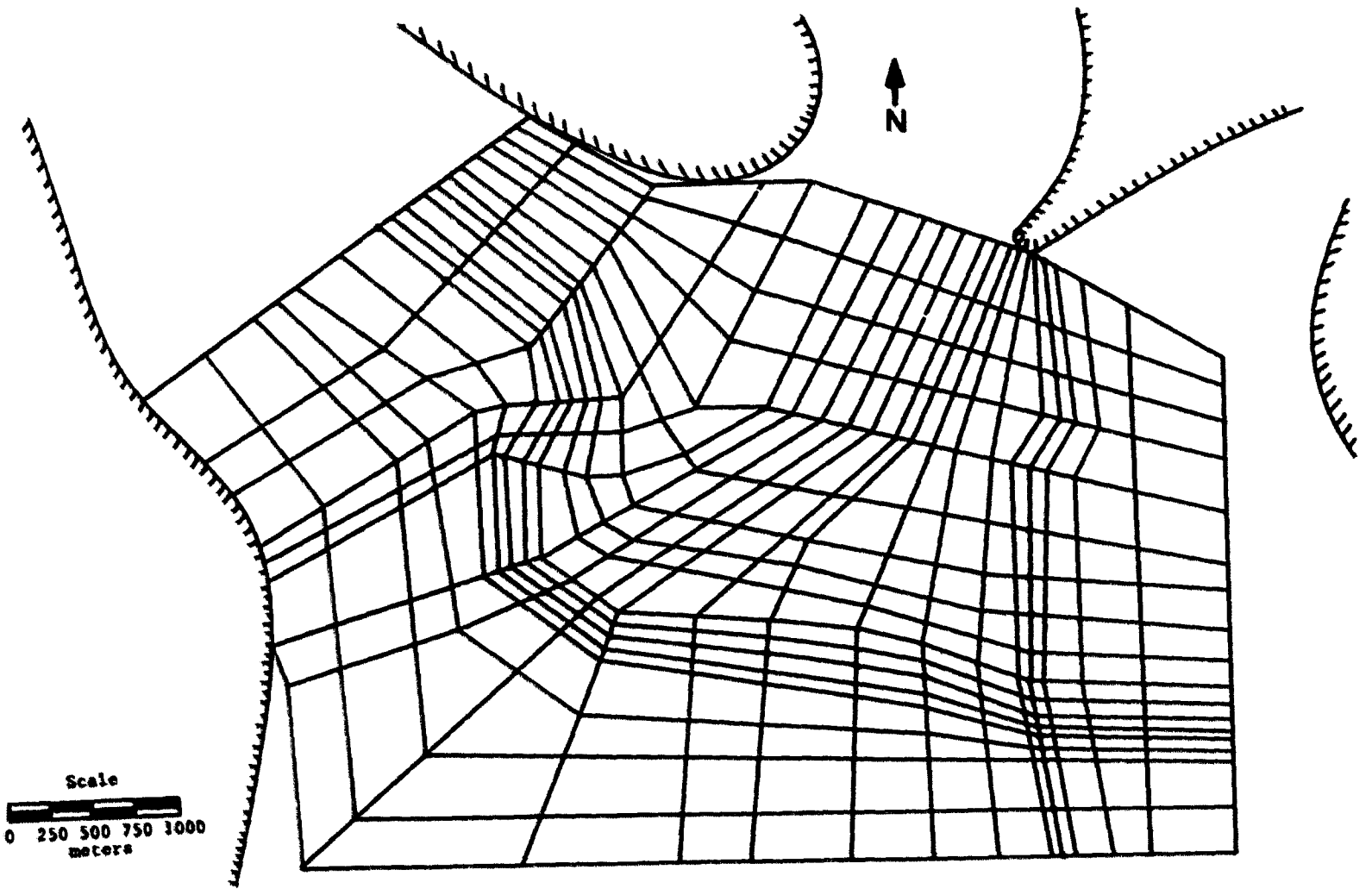

Figure 10. Finite element mesh of Ames aquifer

Initial aquifer hydraulic conductivities were not altered significantly in the Downtown Well Field calibration. The calibration procedure consisted mainly of varying the storage coefficient to achieve the correct timing of drawdown (Table 6).

Table 6. Calibration to Akhavi (1970) Pumping Data

well	3hr		13hr		60hr		
	obs. (m)	SAFEM2 (m)	obs. (m)	SAFEM2 (m)	obs. (m)	SAFEM2 (m)	Error (m)
ow1	0.34	0.14	0.88	0.47	1.07	0.51	-.56
ow2	0.46	0.78	1.34	1.17	1.68	1.24	-.44
ow3	1.59	1.82	2.35	2.21	2.59	2.30	-.29
ow4	1.98	2.28	2.50	2.73	2.71	2.87	+.16
ow5	2.16	1.22	2.68	1.72	2.80	1.94	-.86
ow6	0.79	0.42	1.13	0.66	1.28	0.74	-.54
ow7	0.73	0.00	0.14	0.19	0.18	0.29	+.11
ow11	0.09	0.00	0.27	0.15	0.34	0.32	-.02
cw2	1.59	1.29	2.10	1.75	2.23	1.94	-.29
cw5	2.20	2.15	2.68	2.64	2.84	2.81	-.03
cw7	1.47	1.09	1.98	1.47	2.10	1.58	-.52
cw8	0.82	0.63	1.16	1.00	2.10	1.06	-1.04
cw9	3.60	2.51	4.05	2.96	4.24	3.11	-1.13
cw10	7.87	2.72	8.35	3.16	8.57	3.29	-5.28
cw11	1.04	0.83	1.28	1.19	1.55	1.27	-0.23

The simulation was not particularly effective early in the pumping test but improved with time. The pattern of drawdowns was also not very even throughout the calibration because some observation wells showed an over-estimate of drawdown early in the simulation and an under-estimate of drawdown late in the simulation. The fact that most drawdowns at the 60 hour level are under-estimated is mainly because of

attempts to achieve a reasonable estimate of drawdowns early in the simulation. Further, the Downtown Well Field was close to the northern boundary of the model and was therefore adversely affected by the artificial boundary conditions imposed there. The boundary conditions imposed during the Downtown Well Field calibration was that of a perfect recharge boundary, which accounts for the fact that the long-term drawdowns tended to be slightly less than those observed. The coarseness of the mesh in the downtown area was another reason for the poor model results early in the simulation. The errors at the 60 hour level were acceptable except in city wells 8, 9 and 10. The reason for these discrepancies was because City wells 9 and 10 were pumped wells and thus the averaging process of the numerical model gave smaller drawdowns than observed. City well 8 lies within a pumped element and thus displays a similar error in drawdown. Using a procedure described by Trescott et al. (1976) modified for finite element models, estimated drawdowns in city wells 9 and 10 were 5.26m and 5.44m, respectively. The two wells were combined in one element in the numerical simulation so the estimated water level (5.35m) was closer to the average of the two observed values (6.41m) than unmodified values. A program to estimate the drawdown in a pumped well based on the procedure by Trescott (1975) is included in the model package.

The final value of storage coefficient was 0.0001 which was well within the range reported by Akhavi (1970) of 0.00015 to 0.000075. Hydraulic conductivities were as reported by Drustrup (1985).

Calibration to the Southeast Well Field data necessitated the modification of both storage and permeability values. The pump test data tended to be somewhat difficult to analyze in this area (Drustrup, 1985) because of the extremely high hydraulic conductivities and small drawdowns. Numerical models are difficult to apply accurately to unconfined systems throughout the entire pumping test because of the phenomenon of delayed yield. The parabolic equation describing the flow of groundwater assumes that all releases from storage in the aquifer are instantaneous (i.e. waves propagate at infinite speed in the medium) which is not true in the unconfined case. In the early part of pumping, the rate of fall of the water table may be faster than the rate at which pore water can be released. Thus, the water level will drop quickly and then appear to level out. Once enough time has passed for the pore water to drain, water table levels decline at a steady rate once again. The water then comes from storage in the aquifer. Data from the Asgrow pumping test exhibited the delayed yield response. Since the purpose of the simulation was to test the ability of the aquifer to withstand long term withdrawals, the Asgrow best-fit parameters were optimized for the long term

effects of pumping and thus do not follow the early portion of the drawdown curve particularly well (Figure 11).

The final hydraulic conductivity used in the Southeast Well Field was 2.356mm/s which agrees with the analysis of Drustrup (1985). The final Storage Coefficient of 0.035 is well within the acceptable range of values for an unconfined system and the analysis of Drustrup (1985). The model was seen to fit observed data very well in view of the delayed response phenomenon. It was particularly important to fit these data well because it was in this area that the new well field is proposed.

Verification

During the drought period in 1977, groundwater levels were kept by the City of Ames in several observation wells, thereby providing a long term no-streamflow data set for model verification. A temporary sand dam was placed in the Skunk River downstream of the aquifer recharge point at 13th street. Water was pumped from a gravel pit upstream to recharge the aquifer by providing a constant pool of water above the recharge point. Recharge was continued for a period of one month. The data collected during the recovery period were used for verification of the model. A six-month no-flow simulation was run first to draw the aquifer levels down (pumping rates were duplicated from Austin et al., 1984). Table 7 compares simulated and observed water levels.

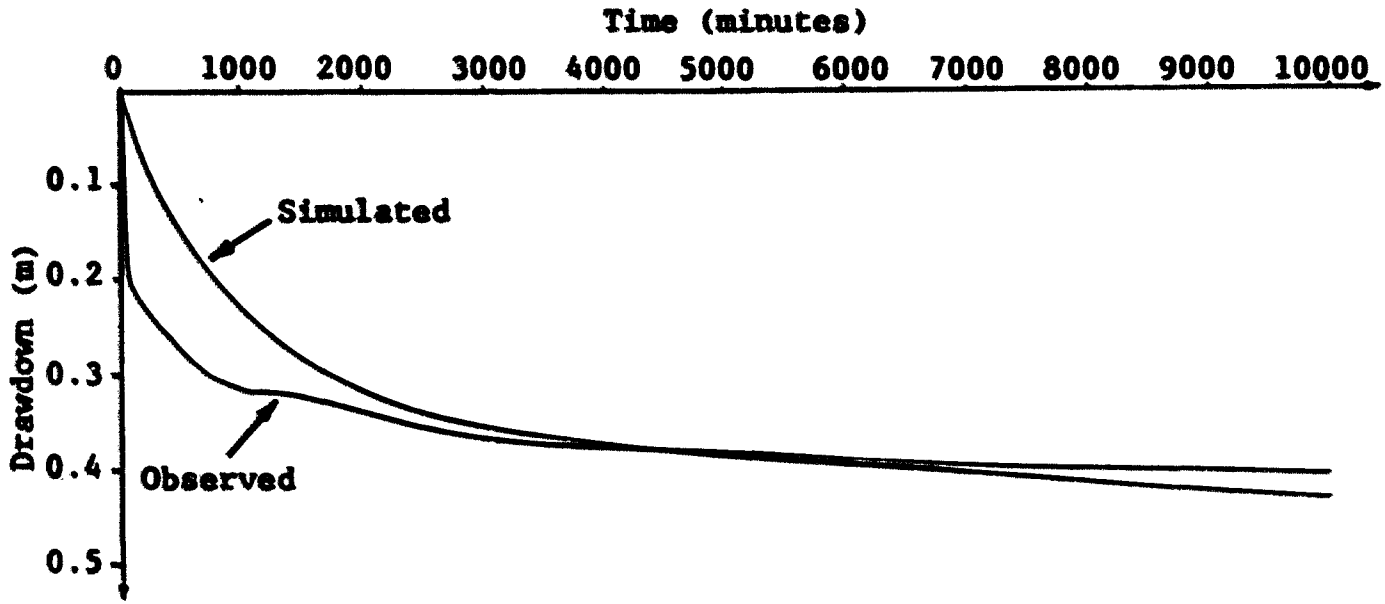

Figure 11. Asgrow pump test calibration

Water levels are quite good once again except in the observation wells close to the northern boundary of the mesh.

Table 7. Water levels at the end of six month no-flow simulation in meters above MSL

Well	Observed (m)	Simulated (m)	Error (m)
ow1	261.16	261.96	-.80
ow2	261.28	261.91	-.63
ow3	260.65	261.11	-.46
ow4	260.75	260.74	+.01
ow6	263.56	261.13	+2.43
ow7	265.66	261.28	+4.38

The low head dam was then inserted in the stream and the model run for one month. Table 8 compares the observed water level rise with simulated values.

Table 8. Groundwater recovery data

Well	Observed (m)	Simulated (m)	Error (m)
ow1	1.45	1.03	-.42
ow2	1.54	1.39	-.15
ow3	2.19	2.31	+.12
ow4	2.81	2.67	-.14
ow6	2.31	5.19	+2.88
ow7	2.05	6.03	+3.98

In general, the model gave excellent recovery values except for Observation wells 6 and 7. The reason for the large discrepancy at wells ow6 and ow7 is that the nodes

representing those wells were close to the northern boundary of the study area and thus were affected by the boundary conditions imposed in much the same way as the Downtown Well Field. During the no-flow simulation, the northern boundary of the model was set as a no-flow boundary to simulate a lack of recharge from the northern part of the aquifer and thus the water levels were depressed lower than necessary. Once the stream carried flow, there was much more recovery in observation wells 6 and 7 because they were now close to a perfect recharge boundary. The average error for wells one to four was only 12.2% which was considered good. The verification was determined to be successful and the model could now be applied to predictive work with some confidence.

Southeast Well Field

To test the performance of the proposed Southeast Well Field, five different pumping configurations were tested with the model.

1. Existing pumping conditions without flow in the Skunk River or Squaw creek.
2. Existing pumping conditions without streamflow plus two 63.1 l/s wells in the Southeast Well Field.
3. Existing Pumping Conditions, two 63.1 l/s wells in the Southeast Well Field plus a low-head dam at 13th Street.
4. Configuration 1 with normal streamflow.
5. Configuration 2 with normal streamflow.

Each simulation was run for a six month simulation

beginning with normal water levels. Figures 12-16 show the drawdown levels for scenarios 1-5, respectively. Results obtained from the simulations indicated that the Southeast Well Field would easily be able to supply water to the city for future needs. Figure 12 (scenario 1) shows that significant drawdowns occur in the Downtown Well Field and in wells located near Iowa State University in the upper left corner of Figure 12. When the Southeast Well Field is added to the simulation (Figure 13) there is a significant 'bowing' of the 6 meter drawdown contour which indicates that the inclusion of the Southeast Well Field does affect drawdowns in the other well fields if no streamflow exists.

When the low-head dam is placed in the system (Figure 14) there is significant recharge to the well fields. Recharge extends throughout the entire system and even affects the Southeast Well Field. Thus, the low-head dam scenario indicated that if water could be pumped from the gravel pit upstream, then during extended low-flow periods, rotating pumping from existing well fields with the low-head dam recharging the system from upstream would sufficiently increase aquifer yields.

If flow was present in the Skunk River and Squaw Creek (both modeled as perfect recharge boundaries) then there was very little drawdown in either the Downtown or Southeast Well Fields (Figures 15 and 16). The addition of the Southeast

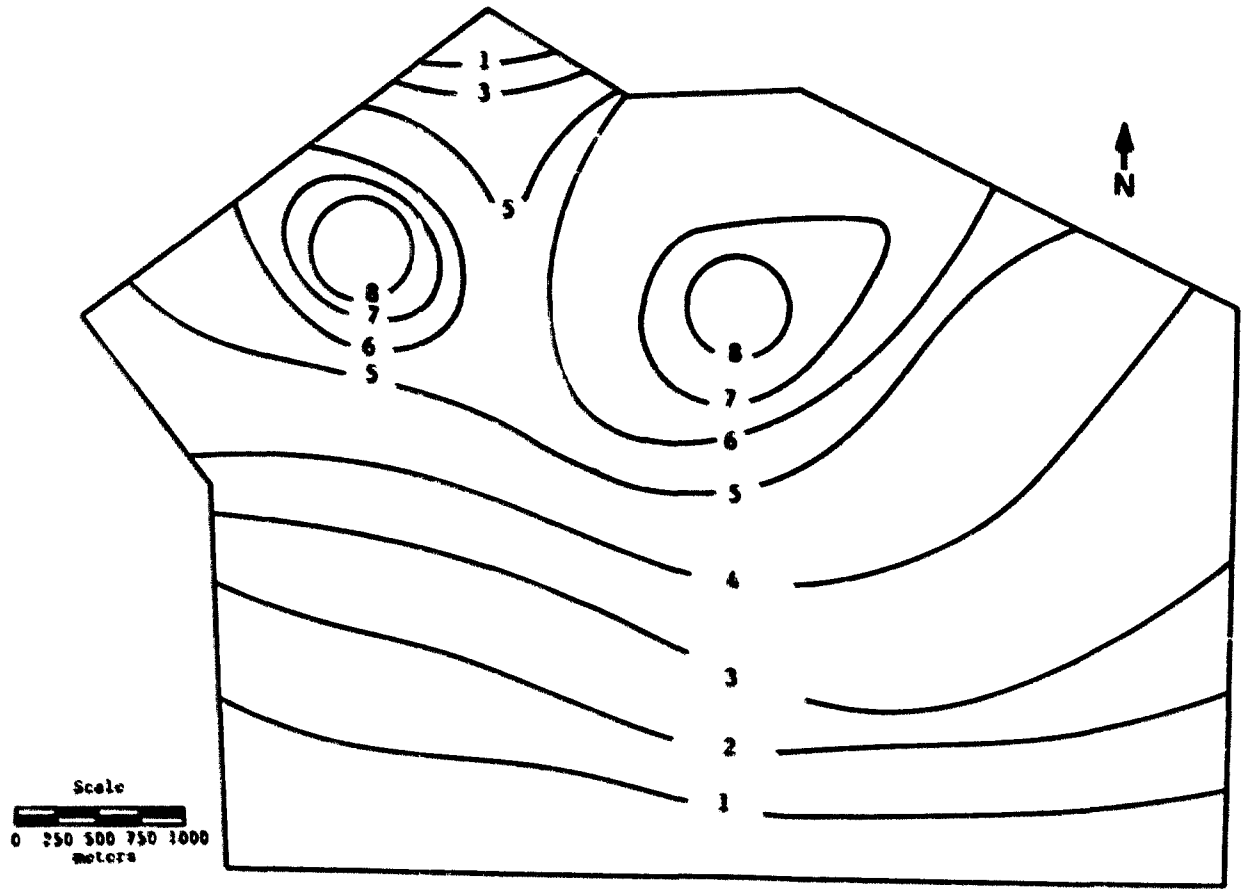

Figure 12. Drawdown in meters for Ames scenario #1

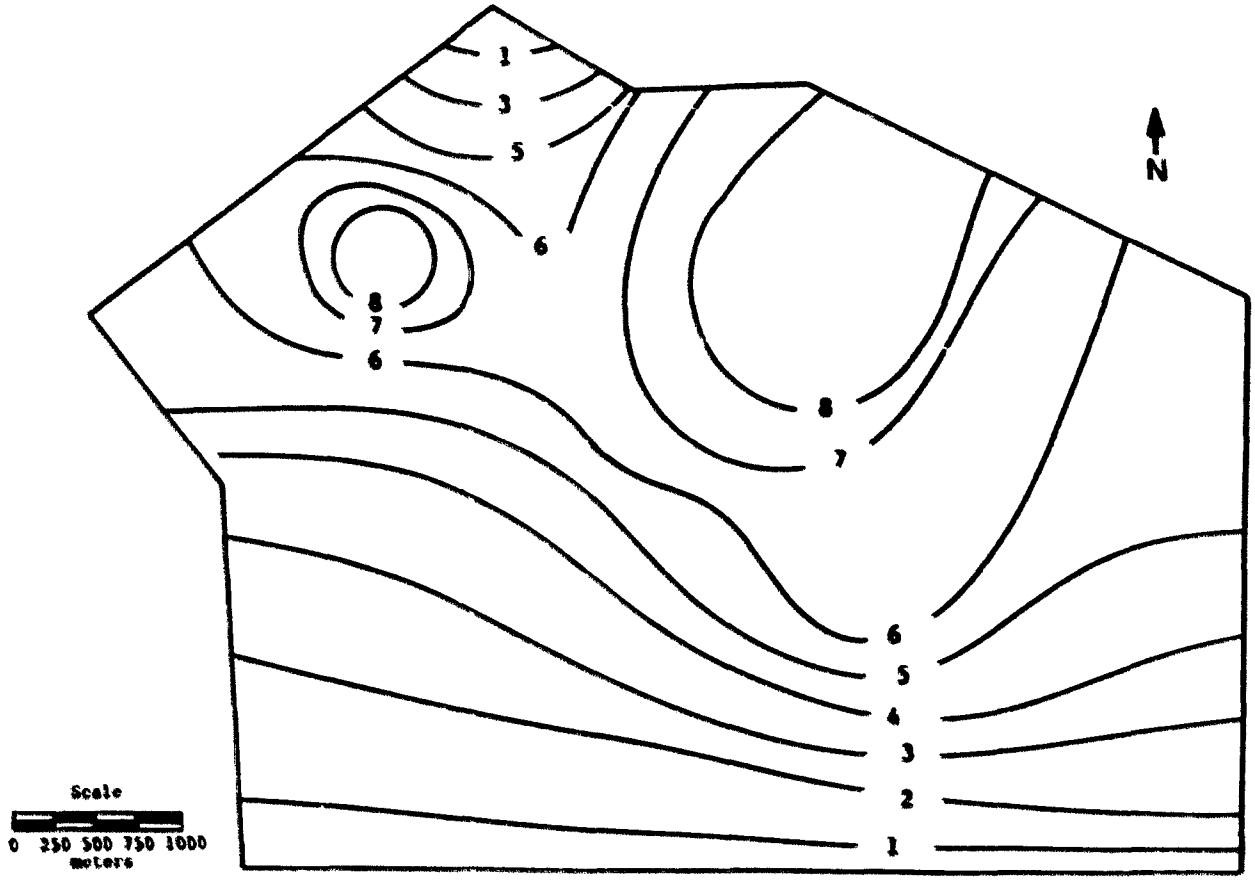

Figure 13. Drawdown in meters for Ames scenario #2

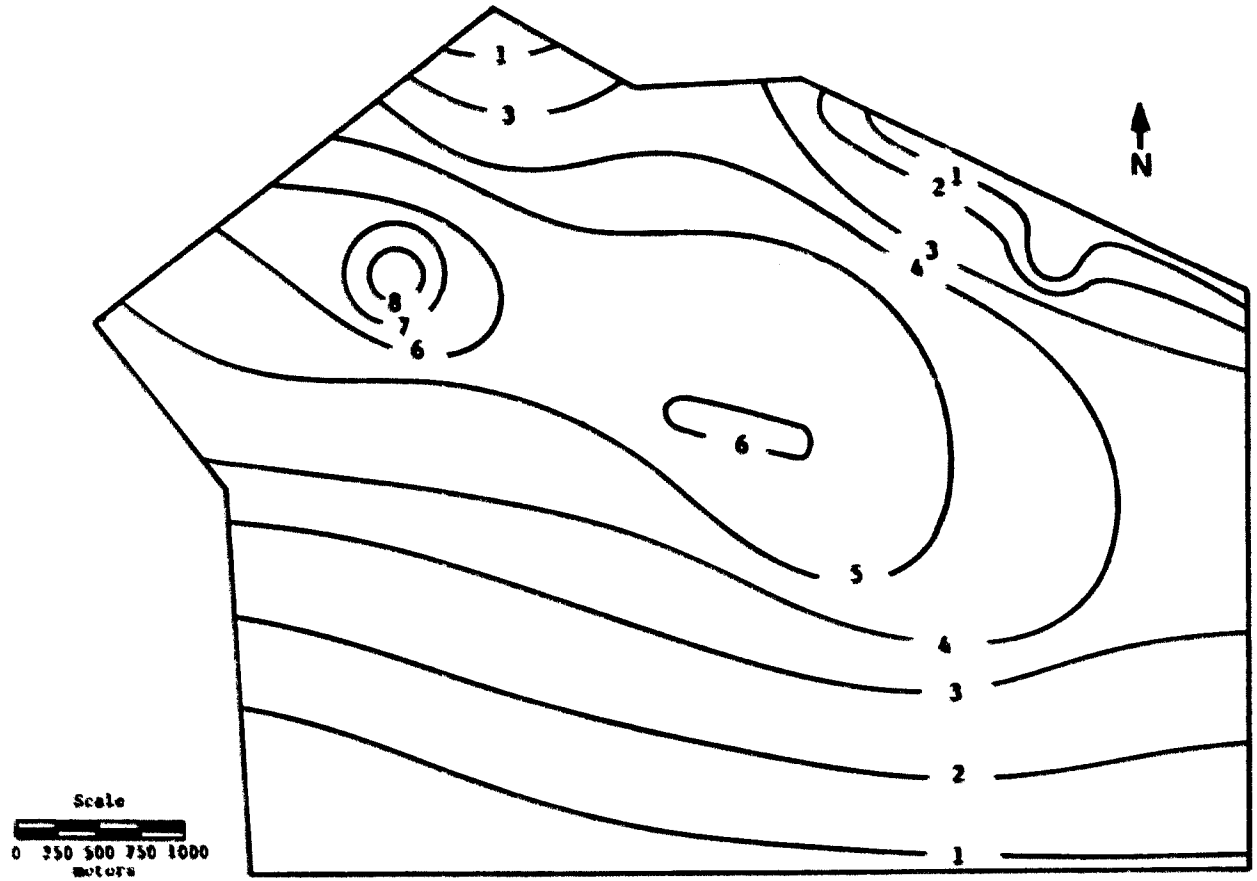

Figure 14. Drawdown in meters for Ames scenario #3

Well Field pumping did not seem to affect the drawdowns in the Downtown Well Field to any significant extent. It was determined that all the flow to the wells was coming from the rivers. If sufficient flow existed in the streams to supply water to the wells, then the Southeast Well Field could be used for large amounts of pumping.

Conclusions

The application of SAFEM2 to the Ames aquifer system was successfully completed including calibration, verification and predictive work. Thus, the micro-computer based model was determined to be a viable groundwater analysis tool. The calibration in the confined portion of the aquifer was not particularly successful mainly because of the close proximity of the wells to the model boundary. The results would certainly improve if the mesh was altered to provide more detail in the downtown area and to better approximate the northern boundary of the aquifer. Because of memory restrictions on the computer used for the simulations, this could not be achieved without removing elements from the Southeast Well Field. Since the purpose of the study was to observe drawdowns in the Southeast Well Field, it was considered acceptable to have reduced accuracy in the downtown area.

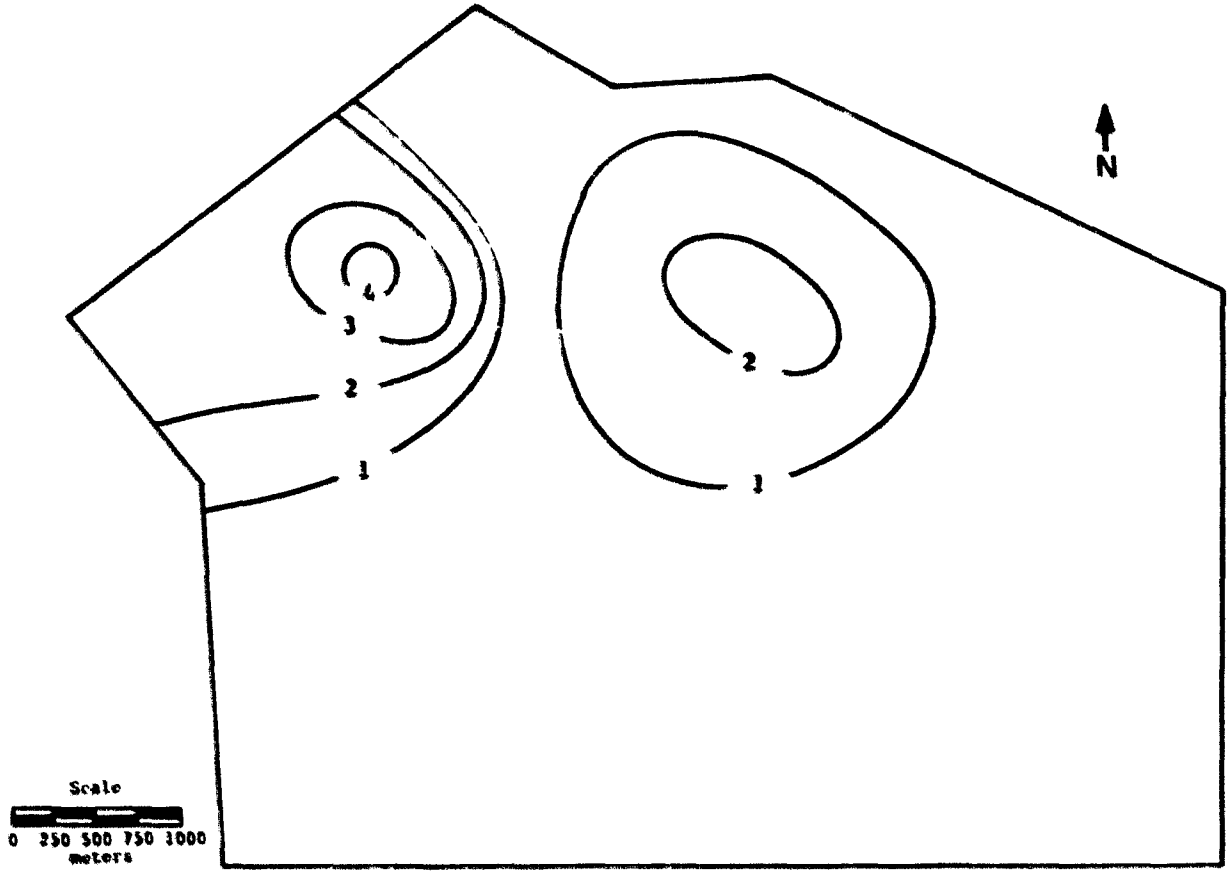

Figure 15. Drawdown in meters for Ames scenario #4

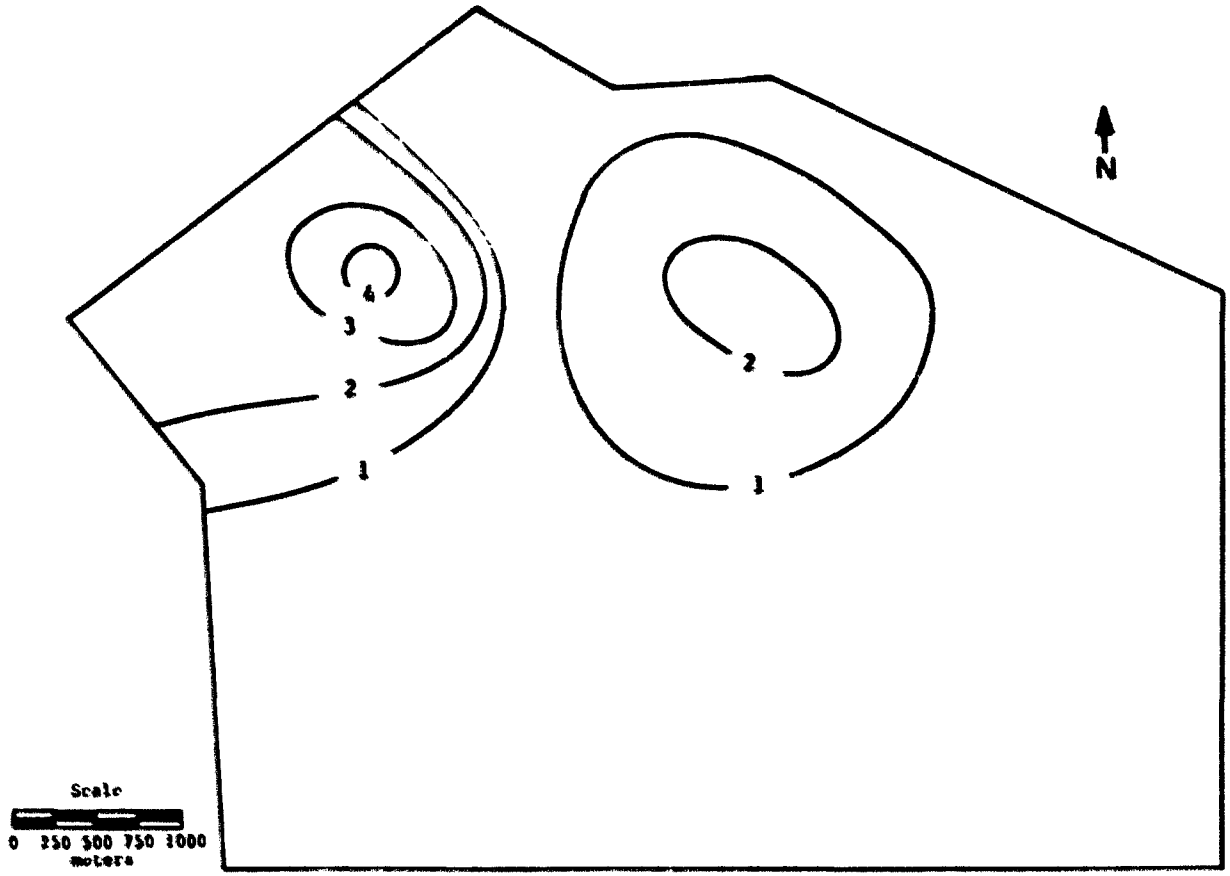

Figure 16. Drawdown in meters for Ames scenario #5

Recommendations

The main problem with applying the model to such a large system was the presence of artificial boundary conditions. With a greatly increased number of nodes, an area large enough to nullify boundary effects could be covered. The machine used for the Ames simulation (IBM PC-XT with 8087 numeric co-processor) was equipped with only 256 kilobytes of RAM (Random Access read/write Memory) which was not really enough to completely cover the Ames Aquifer with a fine mesh. Computers of the type for which the models were written are capable of memory expansion up to 640 kilobytes. Such a memory capacity would enable twice the number of nodes to be stored in the machine and thus improve the accuracy of the model. It took approximately half a second to perform the integrations for each element and place the appropriate values in the arrays. Thus, the assembly time for the mesh used in the Ames simulation was approximately 170 seconds. Depending on the boundary conditions, the time to factor the resulting matrix was approximately 180 seconds which is longer than the actual assembly process. If the model was simulated as a confined system then the solution time was only 10 seconds because the matrix is factored only once.

For the six month simulations used in the Ames analysis, an eight to ten hour time period was required for simulation. This is not an unreasonable amount of time for a small

computer, and actually corresponds to the time the machine would be left idle overnight in a working environment. Thus, the two dimensional model was determined to be an effective and viable groundwater analysis tool in the micro-computer environment.

THREE DIMENSIONAL MODEL

In order to calibrate the three dimensional model (SAFEM3), a test site had to be chosen so that there was significant surface water and groundwater interaction with variation in three dimensions within the aquifer. It was decided that a location close to the junction of the Skunk River and the Squaw Creek would provide true three dimensional variation. An additional requirement was that the stream stage could be measured accurately. A perfect site existed within the Ames aquifer area near an unused stream gauge near the junction of South 16th Street, Ames and the Skunk River (Figure 17).

Study Area

The study area covered an area bounded by US Highway 30 to the south, the Skunk River to the east, Squaw Creek to the north and a distance of 250m to the west. A well had been drilled 250m west of the Skunk River in the South 16th Street road ditch for an earlier study which served as the west boundary. The vertical extent of the mesh extended from the bedrock base of the aquifer to the top of the sands and gravels.

The geometry of the test site is shown in detail in Figure 18. Three piezometers were installed in the aquifer close to the stream gauge so that stream and groundwater

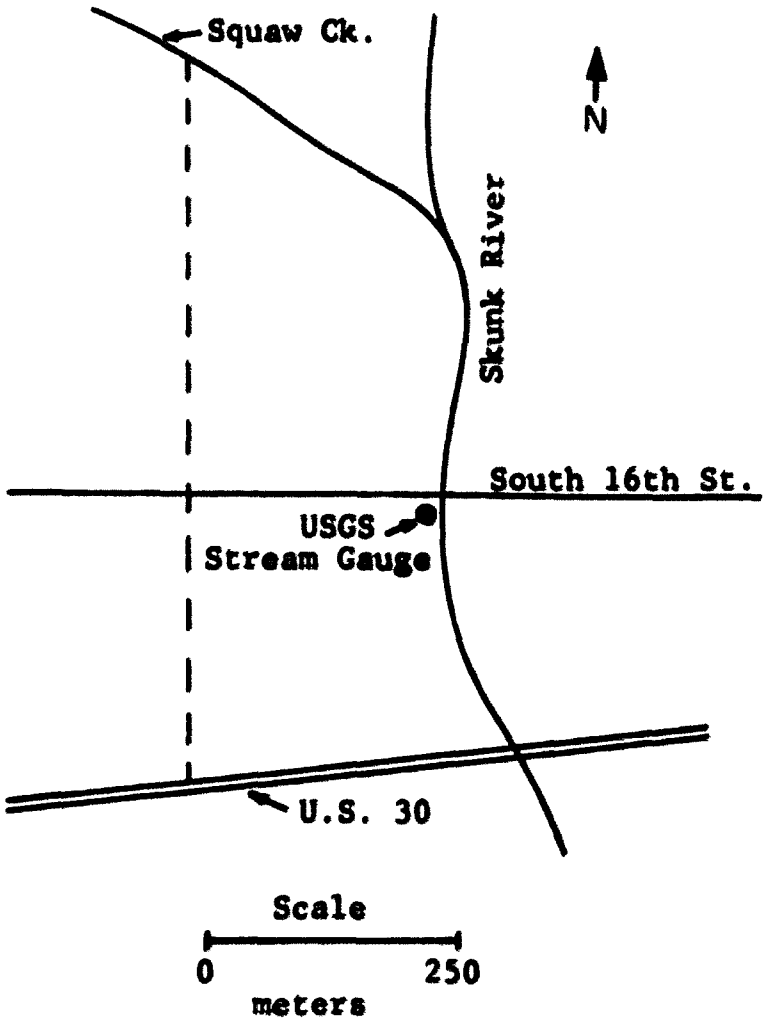

Figure 17. Location of three dimensional study area

levels corresponded closely. The piezometers were each installed to different depths (Figure 19) so that the vertical variation in groundwater levels could be observed under different streamflow conditions. The piezometers were installed to depths of 9.45m, 17.1m and 24.7m. The choice of depths was determined by first drilling the deepest hole to the shale base of the aquifer and then inspecting the well log

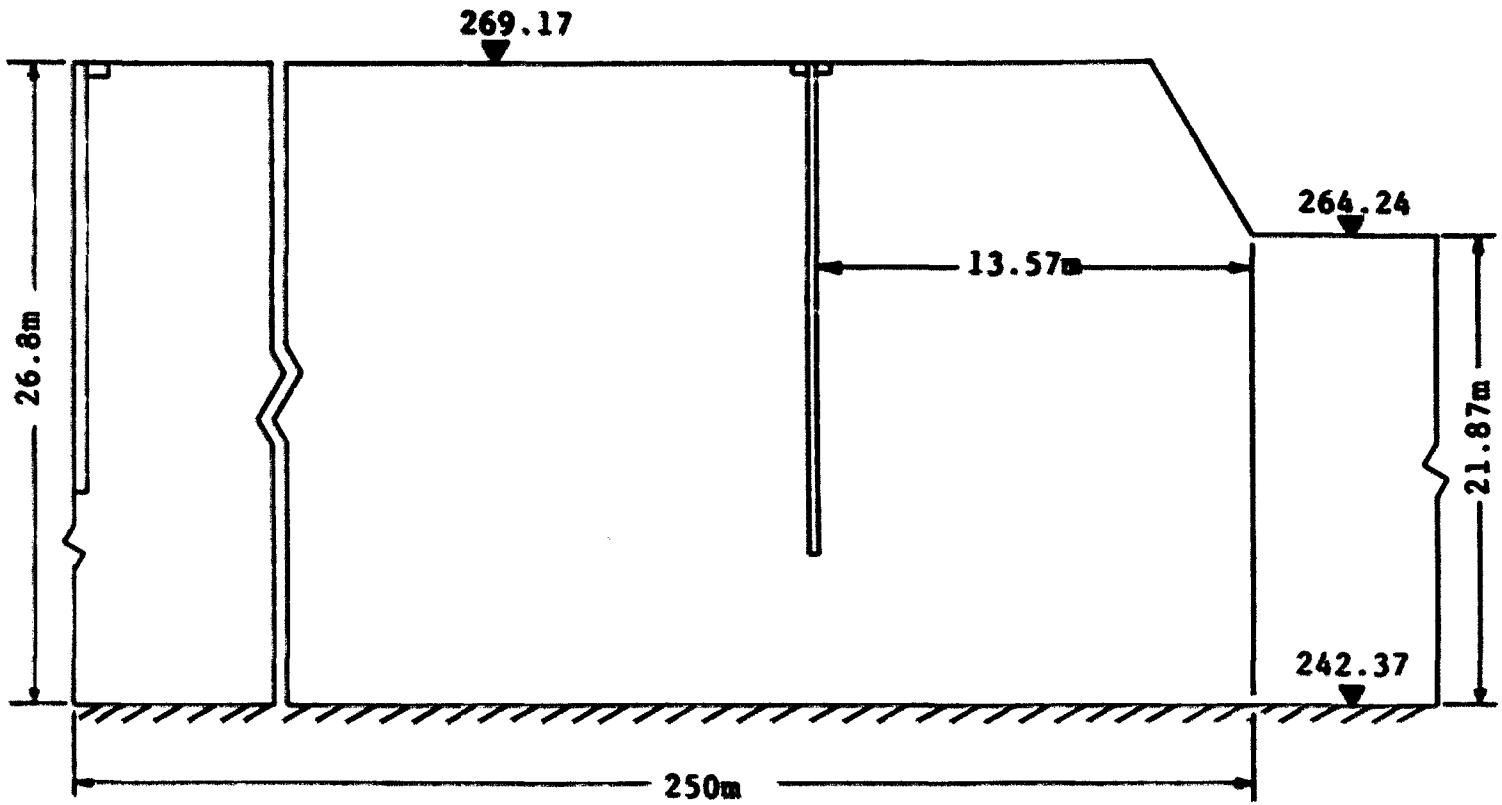

Figure 18. Detail of the three dimensional study area

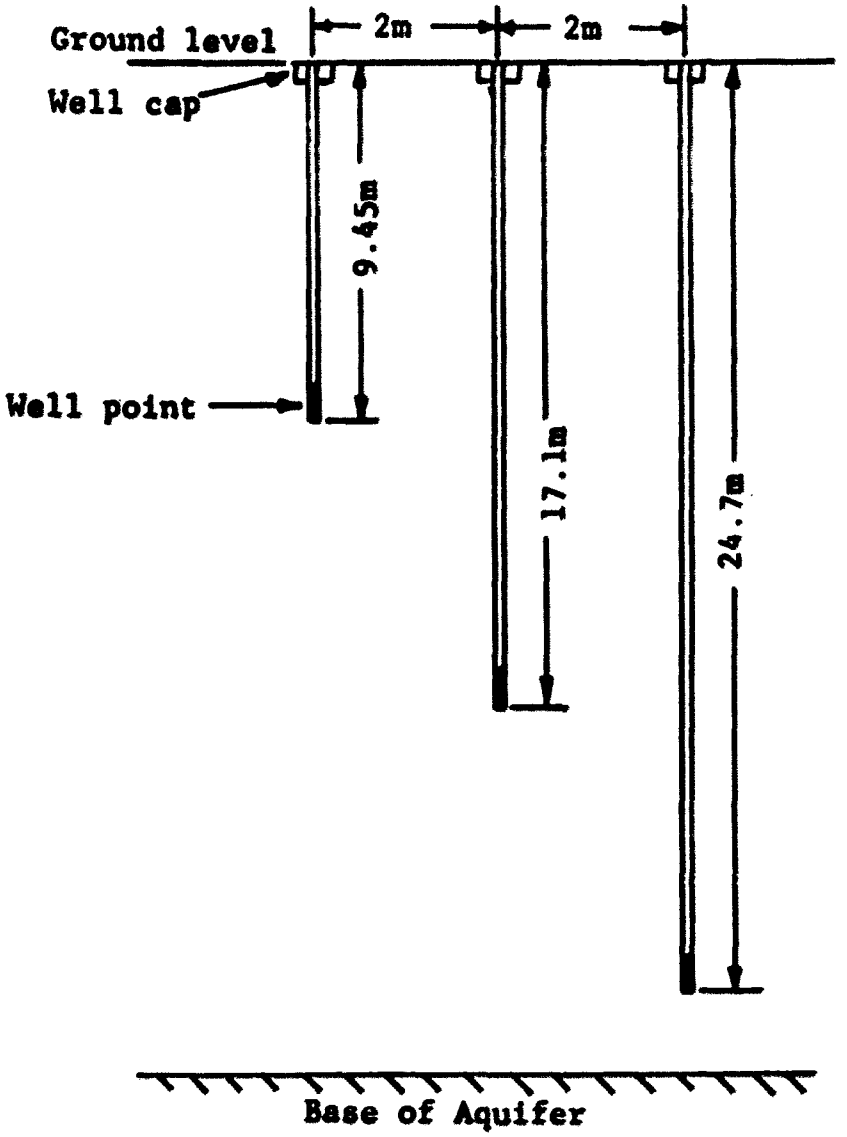

Figure 19. Detail of piezometers for three dimensional study

to determine the water-bearing strata in the aquifer. The deep piezometer well log is contained in the Appendix. The piezometer depths were then selected to be in the coarser layers because most of the groundwater flow would occur in those layers. The piezometers were constructed from 51mm inside diameter PVC pipe with a well point installed at the ends. The well points contained 610mm of slots. The well points were surrounded by pea gravel and sealed one meter above the well points to prevent interference.

Rainfall was not measured directly at the site because the Ames Sewage Treatment Plant (located less than 1km from the test site) kept accurate rainfall records. The stream gauge was easily accessible and in good condition so water levels in the stream could be accurately measured.

Three Dimensional Pump Test

A pump test was attempted to estimate the vertical parameters in the aquifer for the calibration. An air-lift pump was inserted in the center well and drawdowns observed in the shallow and deep wells (Table 9).

It was thought that the data were not useful for two reasons. First, the drawdown data collected for the shallow well show considerable variation in level. This was mainly because of the 'surging' by the air lift pump. The air lift pump works on the principle that air pumped into the well will displace water and therefore force water out of the system.

Table 9. Pump test drawdown data

Time (secs)	Deep well Drawdown (mm)	Shallow well Drawdown (mm)
30	20	43
90	20	55
150	24	40
210	28	10
270	28	28
330	26	28
780	27	40

The bubbling effect of the air caused the water to come out in spurts at irregular times which made estimation of the flowrate very difficult. The average of many measurements was approximately 0.87 l/s. The system was so responsive to withdrawals that the surging affected the measurements. The deeper well was not affected to such a large extent because it was close to the no-flow lower boundary rather than the free surface. The second reason for the data being difficult to analyze was that the drawdowns were extremely small. The equipment used to measure the drawdowns is accurate to about a centimeter which was of the order of the drawdowns in the deep well, thus experimental errors could be large with respect to the drawdown readings. Furthermore, the readings require a few seconds to take which was considered a significant time with the water level changing so quickly.

Calibration to Low-Flow Data

A three dimensional mesh was applied to the test area. The mesh contained 224 nodes and 126 elements. Figure 20 shows the horizontal mesh pattern and Figure 21 shows a typical vertical pattern in the vertical plane. The node numbers indicated on Figure 21 are those corresponding to the location of the observation wells. The potential at the three piezometers was estimated by linear interpolation between nodes 101, 109, 117 and 125. The stream was simulated by a fixed head boundary condition at node 128 in Figure 21.

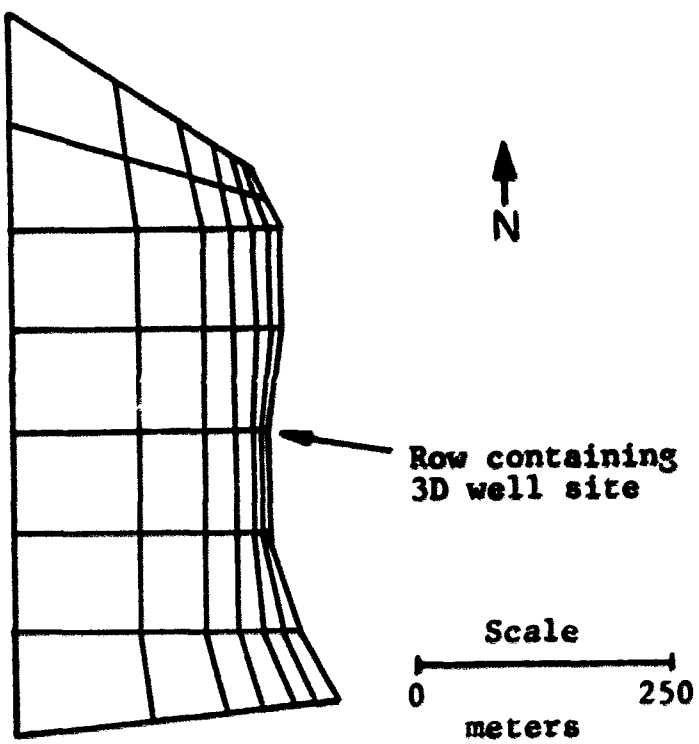

Figure 20. Three dimensional mesh in horizontal (x-y) plane

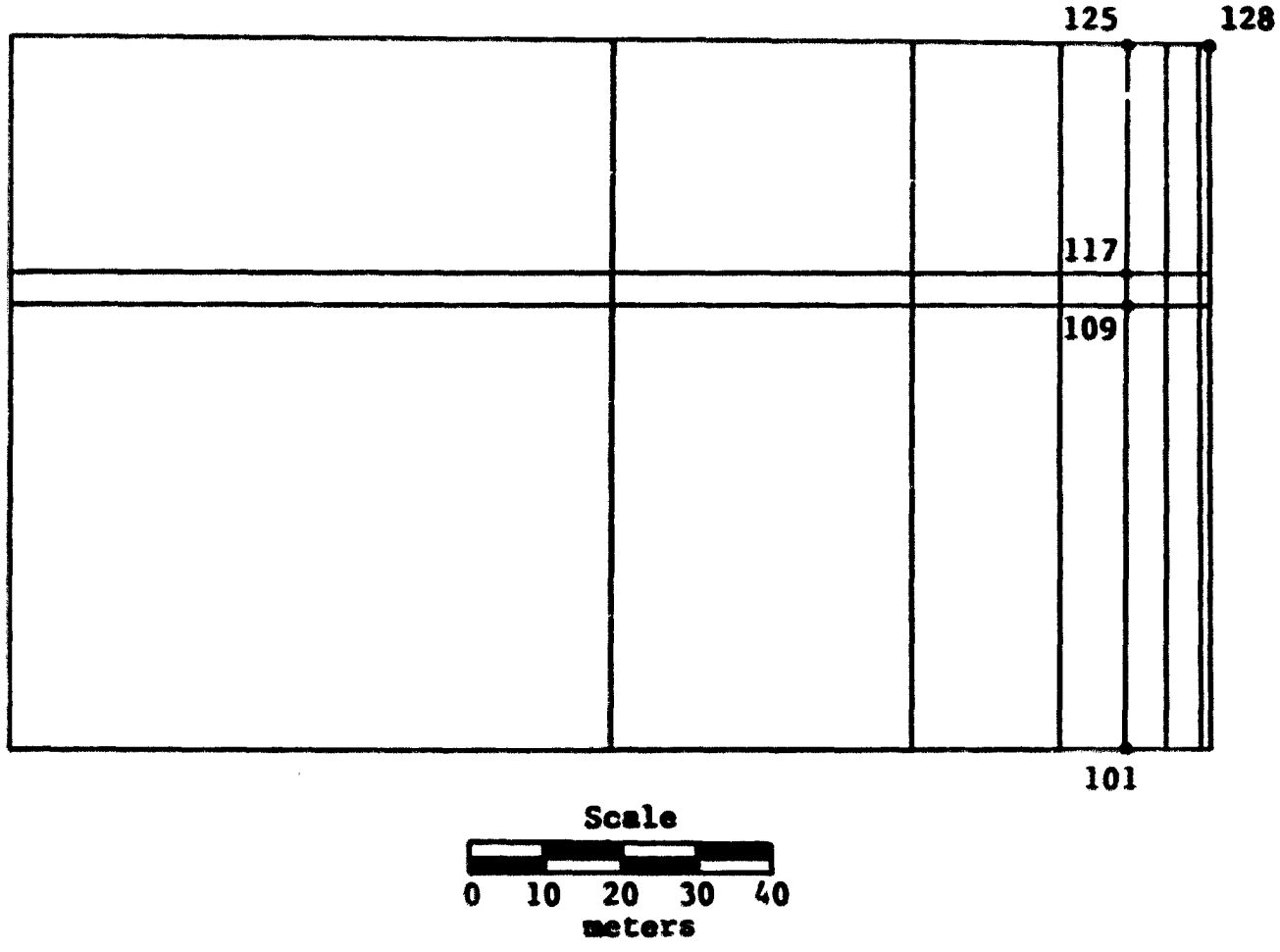

Figure 21. Cross section of three dimensional mesh in East-West direction

The three dimensional model was first calibrated using a set of groundwater level and stream flow level data collected during a dry period in July-August, 1984. There had been a flood in the Ames area in May-June, 1984 so the groundwater levels were very high. The sequence of data collected in July-August, 1984 represented a long 'recession limb' of groundwater flow. The groundwater was discharging into the streams during this period of scarce precipitation which is why neither stream was completely dry. August of 1984 was one of the dryest on record (only 3mm of rain reported) and yet streamflow remained roughly constant.

A six layer model had first been applied to the test site in an attempt to model the correct vertical potential gradients. However, it was found that a four-layered model was just as successful because the controlling factor in the head differentials was the clay lens reported in the well log at approximately 11m. The top and bottom layers of the mesh were assumed to have the same hydraulic conductivity as the two dimensional model (2.356mm/s) and the clay layer hydraulic conductivity would be found through calibration. The model was calibrated to the test data with the vertical variability shown in Figure 22 and with results shown in Figure 23. The clay layer final value of hydraulic conductivity was determined to be 0.04mm/s which falls in the range of fine sands (Bouwer, 1978). This is a respectable value because the

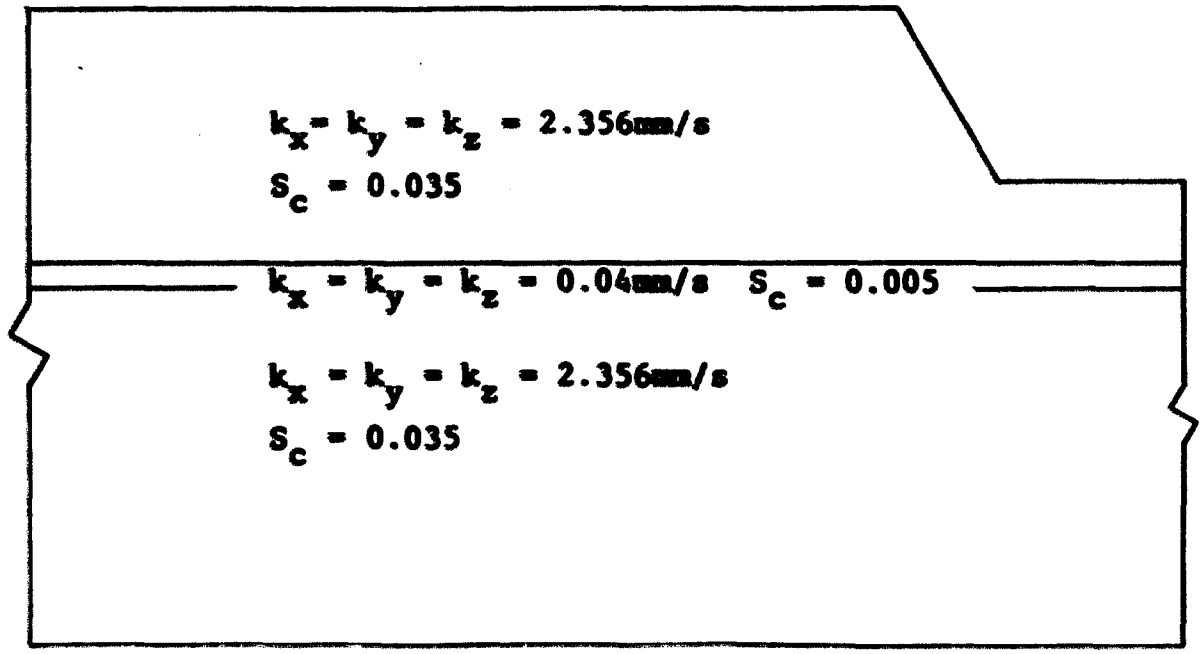

Figure 22. Final calibrated aquifer parameters for low-flow data

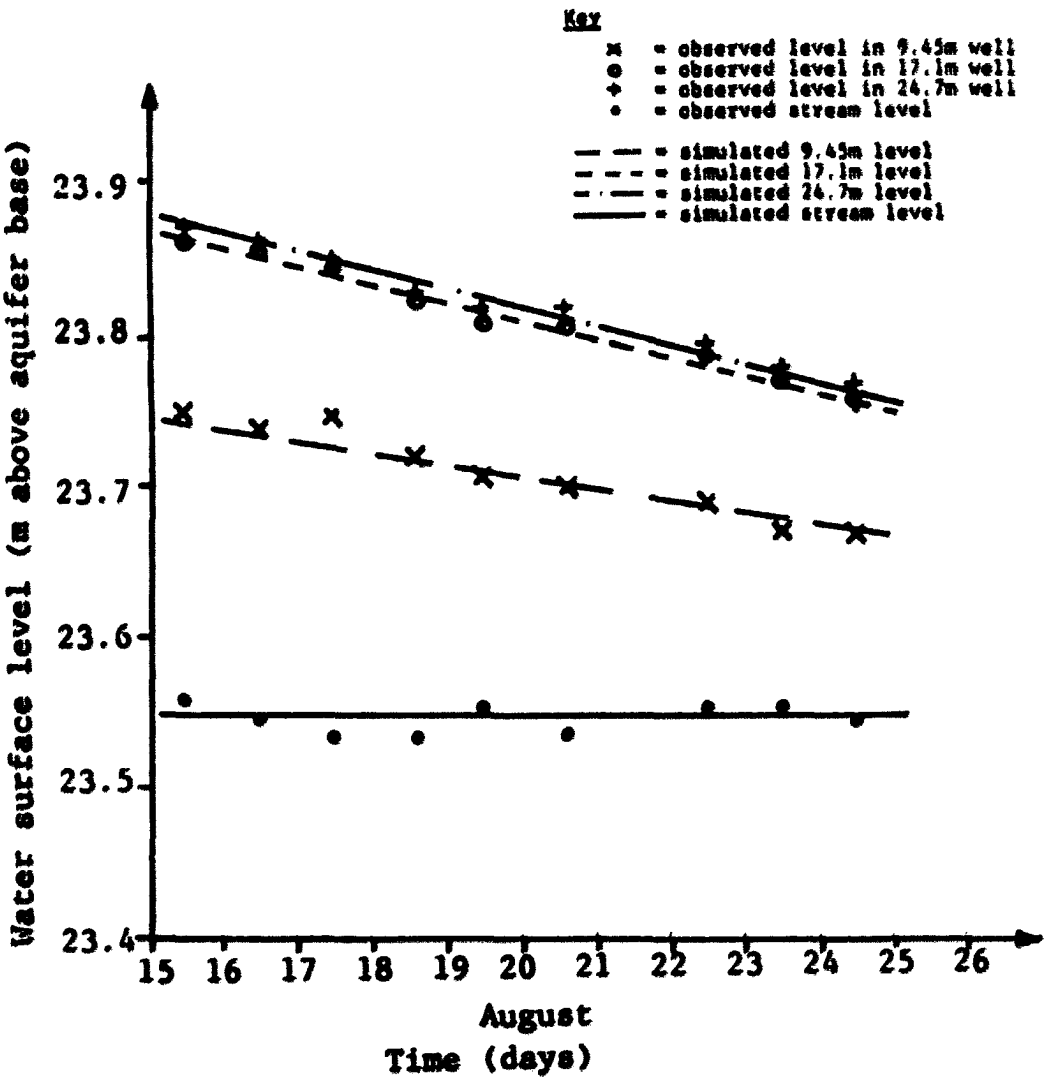

Figure 23. Calibration plot of three dimensional model to low-flow data

clay lens was probably not a full meter thick (the actual thickness was difficult to estimate from the well log) and so a slightly higher hydraulic conductivity over a thicker layer would have the same head loss as a very thin relatively impermeable layer. Furthermore, the layer may not have been entirely clay because well logs are difficult to interpret and only screening samples were taken during the drilling. The stream level was kept constant throughout the simulation as the west boundary was allowed to decrease in water level in accordance with a general lowering of the water table. The results shown in Figure 23 show excellent agreement between observed and simulated water levels. Thus, the calibration to the low-flow data was determined to be successful.

Calibration to Rainfall Data

On October 15th, 1984, a 33.3mm rainfall fell at the test site over a 15 hour time period which produced sufficient change in the streamflow and groundwater levels to allow meaningful data to be taken. The hydraulic conductivities from the recession calibration were used for the aquifer parameters but the model also needed to be calibrated for rainfall events. The soil above the aquifer was Clay loam (U.S. Dept of Agriculture, 1984) and Green-Ampt parameters were chosen from Tables 1, 2 and 3 for clay-loam soils. The initial moisture deficit (IMD) was chosen to be 0.24, the capillary suction parameter was chosen to be 254mm and the

saturated hydraulic conductivity was chosen to be 15mm/s. The 'C' coefficient was chosen to be 50 which would allow nearly all of the rainfall to enter the saturated zone as it came out of the Mein-Larson infiltration model. The stream level and the rainfall were input as the driving forces in the simulation.

The results of the simulation are shown in Figure 24. The influence of the stream level is apparent in the groundwater levels. As the stream level rises, so does the water table by approximately the same amount as the stream. The effect of the rainfall is also apparent as a modification of the rising limb in the 'groundwater hydrograph'. In the early stages after rain began, the infiltration was the controlling factor because the groundwater levels rose and yet the stream level had not begun to increase. The timing of the peak in the groundwater level was not particularly good, but that was mainly because of a lack of accurate data on the stream hydrograph. The recession limb of the groundwater showed a divergence in levels between the deep and shallow wells which was correctly simulated by the model.

The water levels in the horizontal (x-y) plane at the peak of the groundwater hydrograph is shown in Figure 25. The horizontal variability can be seen from the influence of the two streams.

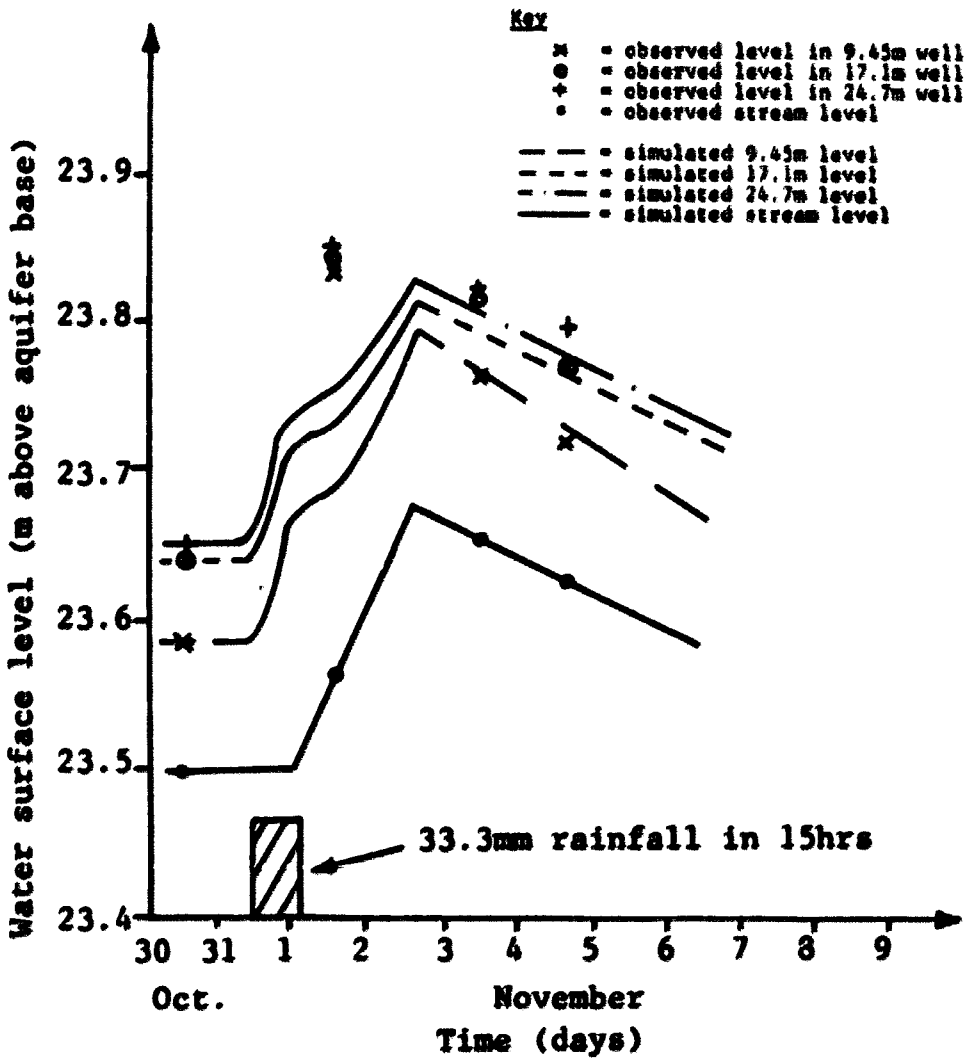

Pigure 24. Calibration plot of three dimensional model to rainfall data

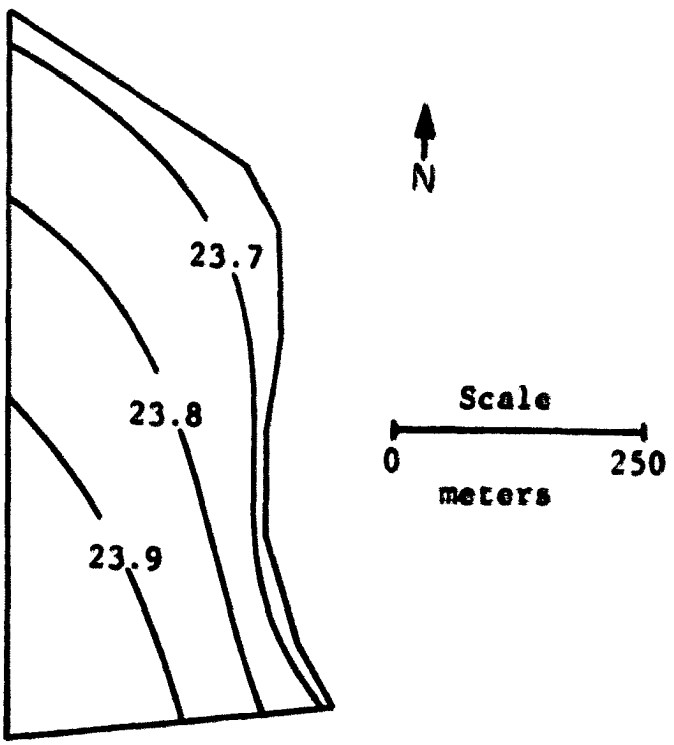

Figure 25. Water table levels at peak levels

A plot of equipotentials at the test site cross-section for the groundwater hydrograph peak is shown in Figure 26. The stream is modeled at the top right hand corner of the cross-section. The effect of the low hydraulic conductivity center layer can be seen in the curvature of the equipotential lines. Significant vertical flow did not seem to take place until very close to the stream. This was probably because of the extremely high horizontal hydraulic conductivity of the aquifer material because even the equipotentials close to the

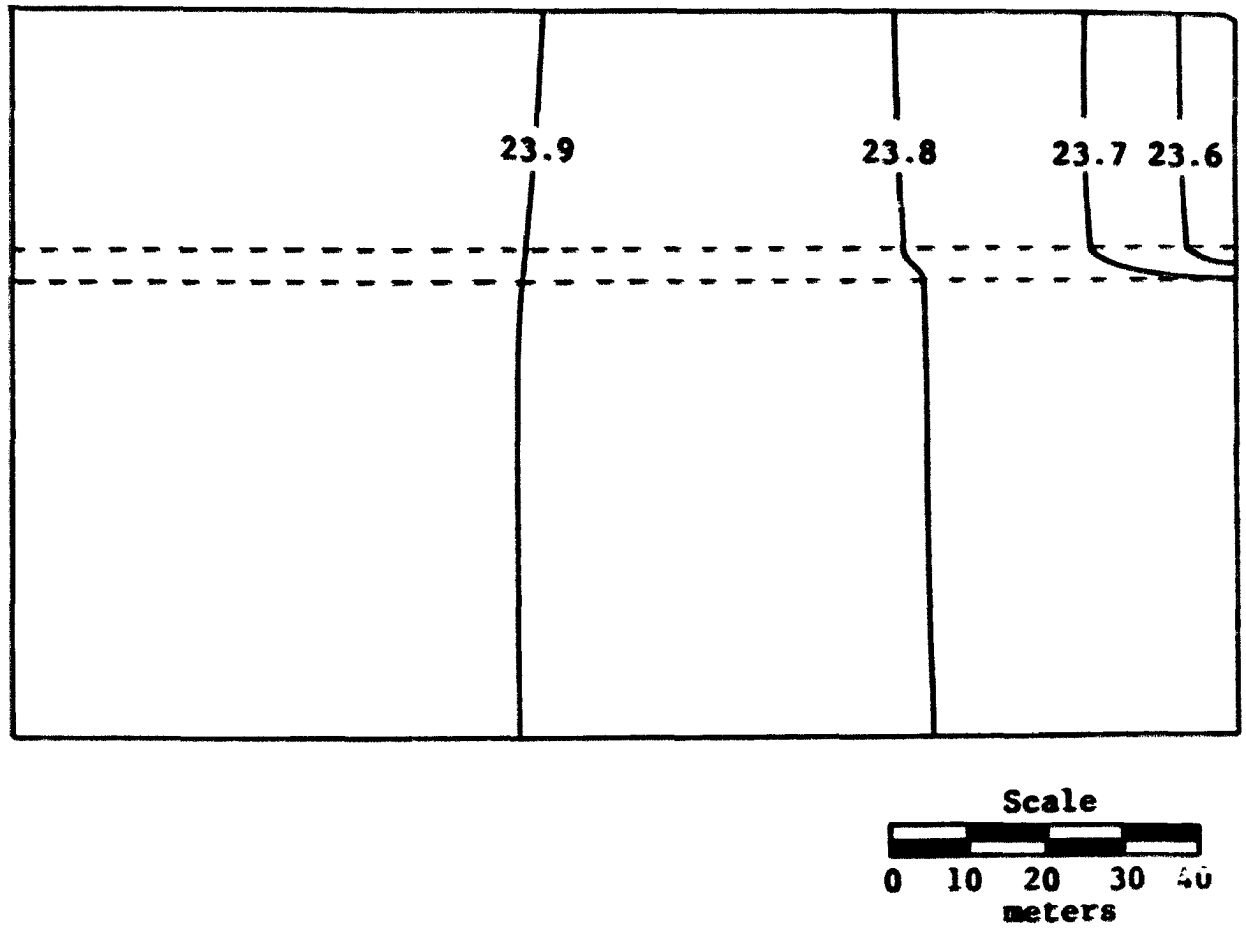

Figure 26. Equipotential plot at groundwater hydrograph peak for East-West cross section

stream show little curvature in the top and bottom model layers. If the horizontal hydraulic conductivities were lower, then water could not be transported in the horizontal direction so easily and more would be transported in the vertical.

Conclusions

The three dimensional model (SAFEM3) was successfully calibrated to two sets of data collected in the Ames Aquifer. The test area was small because unless the aquifer is very deep, the vertical extent of the model becomes very small with respect to the horizontal. Unless a very large number of elements is used, three dimensional work must be confined to small areas. The model produced good results when compared to field data, particularly in low-flow studies.

Recommendations

The usefulness of the three dimensional model for large scale problems must be questioned. The integrations for each element took approximately 2.5 seconds on an IBM PC-XT with an 8087 numeric co-processor. Thus, the matrix assembly process took approximately 310 seconds for the Ames test mesh. Furthermore, the matrix resulting from the fully-implicit finite element procedure has a large bandwidth and is therefore much more storage-intensive than the two dimensional model. The time to factor and solve the matrix used in this

simulation was approximately 300 seconds for a total solution time of 610 seconds for the complete assembly and solution. This time is cut to approximately 330 seconds if the aquifer is considered confined, but can be an extremely large number if the true non-linear equation is solved by iteration. It is therefore concluded that the three dimensional model can be used effectively for small problems where the added detail of vertical flow is required, but the model should not be used for large scale problems on a computer of the size and speed used for this research.

CONCLUSIONS AND RECOMMENDATIONS

Conclusions

The models described in this thesis have been shown to correctly simulate flow in groundwater aquifers with significant surface water interaction. The models offer a significant advance in the state of the art of groundwater modeling by bringing recent advances in the field (deformable isoparametric elements, interactive inputs) to the working community where state of the art models are needed most. The application to the micro-computer is not a significant advance in itself but further adds to the utility of the models.

Recommendations

There are many ways in which the models could be improved, the main one being the implementation of the models on a faster computer. The three dimensional model has great utility but the smaller machines cannot provide enough computational power to make it worthwhile. Fortunately, small desktop machines are becoming more powerful every year so the true utility of the models may not be realized for a few years. The models were written in relatively standard Pascal so conversion to other Pascal dialects should not be difficult. Further improvements would be the ability to use different element types across the domain (including special basis functions in pumped elements), an evapotranspiration

package and allowing the streamflow to be updated from groundwater flow.

Of more importance than the obsession with mathematically exact numerical models is the problem of data collection in groundwater hydrology. It would appear at this point that our technologies far outweigh our ability to estimate field parameters. The problems of anisotropy and inhomogeneity are the real stumbling blocks in our analysis of the real world. The approach currently used is that of parameter averaging over finite areas. It is interesting to note that all of the models currently in existence (including those described in this thesis) are supposedly 'exact', but the calibration process still requires parameter modification for correct results.

The models described in this dissertation will be made available in machine-readable form with a users manual. Information on the availability of the models may be obtained from the Iowa State Water Resources Research Institute, Room 355 Town Engineering Building, Iowa State University, Ames, Iowa, 50011.

REFERENCES

Akhavi, M. S. "Occurrence, Movement and Evaluation of Shallow Groundwater in the Ames, Iowa Area." Ph.D. Dissertation. Iowa State University, Ames, Iowa, 1970.

Austin, T. A., Drustrup, R., Antosch, L., Willie, L. and Parsons, W. W. "Supplemental Water Supply Studies, City of Ames Completion Report." Iowa State Water Resources Research Institute, Iowa State University, Ames, Iowa, 1984.

Bathe, K. and Wilson E. L. Numerical Methods in Finite Element Analysis. Prentice-Hall, New York, 1976.

Bettess, P., and Bettess, J. A. "Analysis of Free Surface Flows Using Isoparametric Finite Elements." International Journal for Numerical Methods in Engineering, 19 (1983), 1675-1689.

Bouwer, H. Groundwater Hydrology. McGraw-Hill Series in Water Resources and Environmetal Engineering, McGraw-Hill, New York, 1978.

Brakensiek, D. L., and Rawls, W. J. "An Infiltration Based Runoff Model for a Standardized 24-Hour Rainfall." ASAE Paper No. 81-2504, 1982.

Chu, S. T. "Infiltration During an Unsteady Rain." Water Resources Research, 14 (1978), 461-466.

Ciarlet, P., The Finite Element Method for Elliptic Problems. North-Holland Publishing Company, Amsterdam, 1978.

Cunningham, A. B., and Sinclair, P. J. "Application and Analysis of a Coupled Surface and Groundwater Model." Journal of Hydrology, 43 (1979), 129-148.

Desai, C. S., and Li, G. C. "Transient Free Surface Flow Through Porous Media Using a Residual Procedure." In Finite Elements In Flow Problems. Proceedings of the Fourth International Symposium on Finite Elements in Flow Problems, Chuo University, Tokyo, July 26-29, 1982, 621-632.

DeWitt, T. A. "Soil Survey of Story County, Iowa." U.S. Department of Agriculture, Soil Conservation Service, Des Moines, Iowa, 1984.

Dougal, M. D., Sendlein, L. V. A., Johnson, R. L. and Akhavi, M. S. "Groundwater and Surface Water Relationships for the Skunk River at Ames, Iowa." Iowa State University Engineering Research Institute, Ames, Iowa, Special Report ISU-ERI-AMES-99984, 1971.

Drustrup, R. "An Analysis of the Proposed Southeast Well Field, City of Ames, Iowa." Unpublished M.S. Thesis. Iowa State University, Ames, Iowa, 1985.

France, P. W. "Finite Element Analysis of Three Dimensional Groundwater Problems." Journal of Hydrology, 21 (1974), 381-398.

Gary, J. "The Numerical Solution of Partial Differential Equations." Unpublished Lecture Notes. Department of Computer Science, University of Colorado, Boulder, Colorado, 1975.

Green, W. H., and Ampt, G. A. "Studies on Soil Physics." Journal of Agricultural Science, 4 (1911), 1-24.

Gupta S. R., and Tanji, K. K. "A Three Dimensional Galerkin Approximation of Flow Through Multi-Aquifers in Sutter Basin, California." Water Resources Research, 12 (1976), 155-162.

Guvanasen, V., and Volker, R. E. "Numerical Solutions for Unsteady Flow in Unconfined Aquifers." International Journal for Numerical Methods in Engineering, 15 (1980), 1643-1657.

Huber, W. C., Heaney, J. P., Nix, S. J., Dickson, R. E. and Polmann, D. J. "Storm Water Management Model." U.S. Environmental Protection Agency, Cincinnati, Ohio, 1982.

Jennings, A., Matrix Computations for Engineers and Scientists. John Wiley and Sons, New York, 1977.

Lapidus, L. and Pinder, G. F., Numerical Solution of Partial Differential Equations in Science and Engineering. John Wiley and Sons, New York, 1982.

McDonald, M. G., and Harbaugh, A. W. "A Modular Three-Dimensional Finite-Difference Ground-Water Flow Model." U.S. Department of the Interior, U.S. Geological Survey, Washington, D.C., 1983.

Mein, R. G., and Larson, C. L. "Modeling Infiltration during a Steady Rain." Water Resources Research, 9 (1973), 384-394.

Merva, G. E., and Fausey, N. R., "Finite Element Analysis of Water Table Observation Well Behavior." Paper presented at the 1984 Summer Meeting of the ASAE, University of Tennessee, Knoxville, Tennessee, June 24-27, 1984.

Morel-Seytoux, H. J., and Khanji, J. "Derivation of an Equation of Infiltration." Water Resources Research, 10 (1974), 795-800.

Neumann, S. P., and Witherspoon, P. A. "Finite Element Method of Analyzing Steady Flow With a Free Surface." Water Resources Research, 6 (1970), 889-897.

Neumann, S. P., and Witherspoon, P. A. "Analysis of Non-Steady Flow With a Free Surface Using the Finite Element Method." Water Resources Research, 7 (1971), 611-623.

Pinder, G. F., and Frind, E. O. "Application of Galerkin's Procedure to Aquifer Analysis." Water Resources Research, 8 (1972), 108-120.

Rawls, W. J. and Brakensiek, D. L. "Green-Ampt Infiltration Parameters From Soils Data." ASCE Journal of Hydraulic Engineering, 109 (1983a), 62-70.

Rawls, W. J. and Brakensiek, D. L. "A Procedure to Predict Green-Ampt Infiltration Parameters." In Advances In Infiltration. Proceedings of the National Conference on Advances in Infiltration, Chicago, Illinois, December 12-13, 1983b, pp. 102-112.

Reddy, J. N., An Introduction to the Finite Element Method. McGraw-Hill, New York, 1984.

Trescott, P. C., Pinder, G. F., and Larson, S. P. "Finite Difference Model for Aquifer Simulation in Two Dimensions with Results of Numerical Experiments." U.S. Geological Survey Techniques of Water Resources Investigations, Book 7, Chapter C1 U.S. Geological Survey, Washington, D.C., 1976.

Willie, L. E., "The Hydrogeologic Investigation of the Southeast Well Field and McCallsburg Arm, Ames, Iowa." M.S. Thesis. Iowa State University, Ames, Iowa, 1984.

Wilson, B. N., Slack, D. C. and Young, R. A. "A Comparison of Three Infiltration Models." Scientific Journal Series Paper No. 11554 Minnesota Agricultural Experiment Station, University of Minnesota, Minneapolis, Minnesota, 1982.

Zienkiewicz, O. C. The Finite Element Method in Engineering Science. McGraw-Hill, New York, 1971.

ACKNOWLEDGEMENTS

The research described herein was funded by a grant from the U.S. Department of the Interior, Geological Survey, grant number G-906-03, and administered by the Iowa State Water Resources Research Institute. Additional support was provided by the Engineering Research Institute, Iowa State University.

The author thanks Dr T. A. Austin for his supervision and kind support throughout the project. In addition, thanks are extended to committee members (in alphabetical order) Dr R. Alexander, Dr C. Anderson, Dr R. A. Lohnes and Dr R. L. Rossmiller for their help and expertise.

APPENDIX :

BOREHOLE LOG AT THREE DIMENSIONAL WELL SITE

Table A.1. Description of borehole log

Depth (m)	Description
0.0-3.0	Black silty river clay
3.0-5.5	Yellow silty clay
5.5-6.1	Medium-coarse gravel
6.1-6.7	Medium-coarse sand
6.7-7.0	Sandy clay
7.0-8.2	Fine sand
8.2-9.1	Fine to coarse sand
9.1-9.6	Clay and sand
9.6-10.7	Sand and gravel
10.7-11.3	Clay lens
11.3-14.3	Sand and gravel
14.3-14.6	Cobbles and coarse gravel
14.6-16.2	Coarse sand
16.2-17.7	Sand and gravel
17.7-18.6	Sand with cobbles
18.6-23.2	Sand and gravel
23.2-24.6	Gravel
24.6-25.0	Yellow clay
25.0-25.6	Clay and gravel
25.6-26.8	Gravel
26.8-27.1	Shale

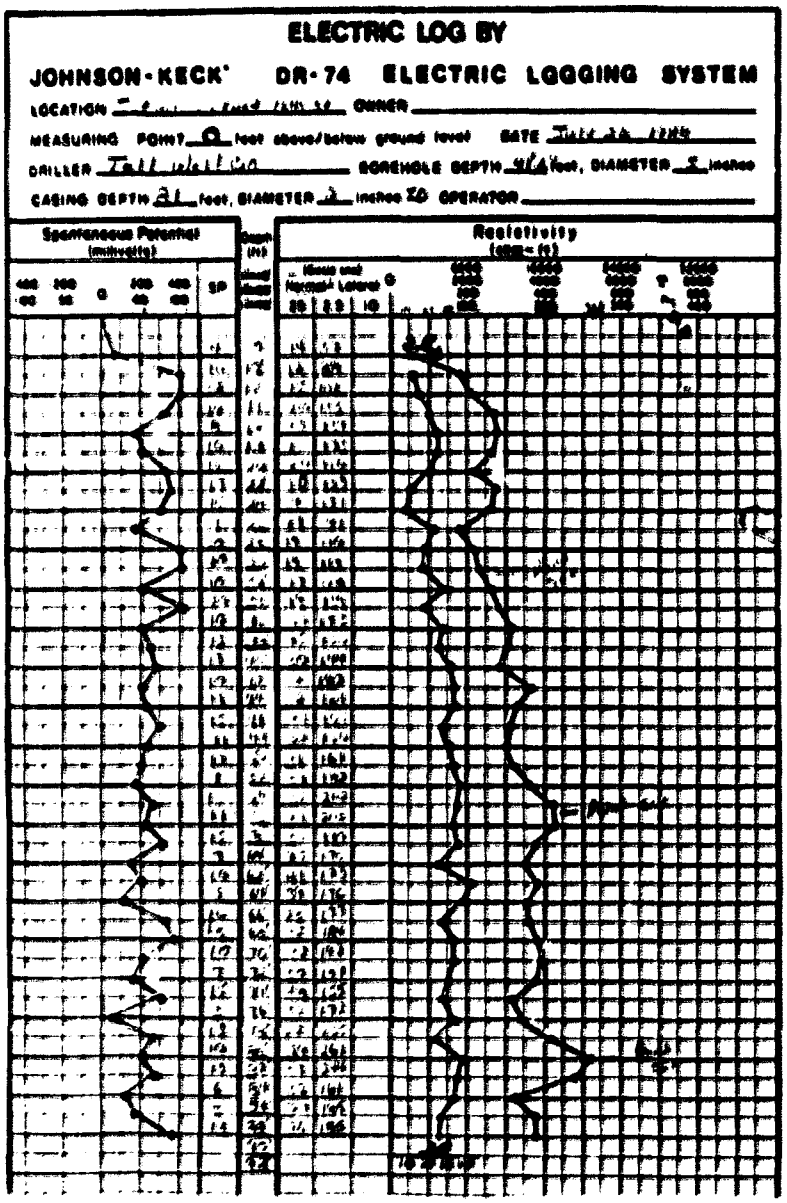

Figure A.1. Borehole log